Designing Subsidies and Recycling Plans for Sustainable Construction and Demolition Waste Treatment

Lei Yu[a], Qian Ge*[b,c], Ke Han†[b], Wen Ji[a], Yueqi Liu[a]

[a] *School of Transportation and Logistics, Southwest Jiaotong University, Xi'an 999, Pidu District, Chengdu, 611756, Sichuan, China*
[b] *School of Economics and Management, Southwest Jiaotong University, No. 111, North Section 1, 2nd Ring Road, Chengdu, 610031, Sichuan, China*
[c] *Department of Civil Engineering, Graduate School of Engineering, The University of Tokyo, 7-3-1 Hongo, Bunkyo-ku, Tokyo, 113-8656, Japan*

Abstract

More than 10 billion tons of construction and demolition waste (CW) are generated globally each year, which has a non-negligible impact on the environment. In the recycling process of the CW, government and the carrier are two main stakeholders. The carrier is responsible for transporting the CW from production sites to backfill sites or processing facilities, whose main concern is the economic benefits and transport efficiency. Meanwhile, the government, as the regulator, focuses on minimizing pollution generated by the recycling system, which is influenced by transport modes, shipment distances, and the types of processing facilities used. This paper develops a bi-level optimization model to address these challenges. The upper-level model optimizes the government's subsidy scheme, while the lower-level model focuses on the carrier's recycling plan. With the introduction of the time-space network, the lower-level model is formulated as a tailored minimum cost flow problem and the upper-level problem as a linear programming model. Due to the complex structure and large number of variables of the problem, we design a hybrid heuristic method. A case study in Chengdu demonstrates that the lower-level model could achieve a gap less than 0.43% within 58 seconds, and the whole problem could be solved with a gap of less than 1.51% within 3.76 hours. Results show that with an optimized subsidy scheme and recycling plan, pollution can be reduced by over 29.29% with a relatively small subsidy investment.

Keywords: Construction and demolition waste; Sustainable treatment; Minimum cost flow problem; Bi-level programming; Hybrid algorithm

1. Introduction

The global urbanization and urban renewal are leading to a significant increase in construction projects. With this comes a large amount of construction and demolition waste (CW), more than 10 billion tons of CW are generated globally annually (Yazdani et al., 2021), making it a major component of municipal solid waste. It accounts for 25-40% in developing and developed countries (Lin et al., 2020). As the largest contributor, China generates more than 3 billion tons of CW annually, the United States generates more than 600 million tons annually, and the European Union generated 372 million tons in 2018 (Huang et al., 2018; Zheng et al., 2024). Despite the enormous number, the recycling rate of the CW is quite small compared with other types of urban waste. In China, only 5% of CW are recycled (Huang

*Corresponding author. Email: geqian@swjtu.edu.cn
†Corresponding author. Email: kehan@swjtu.edu.cn

et al., 2018). Nonetheless, improper treatment can cause serious environmental hazards such as soil contamination and degradation, air and water pollution, greenhouse gas emissions, global warming, and severe health problems (Rathore and Sarmah, 2020). This highlights the need for an efficient, environmentally friendly CW recycling plan.

Three types of sites are integral to the recycling process of CW: production sites, backfill sites, and processing facilities (Chu et al., 2012; Yu and Han, 2025; Yazdani et al., 2021). The contractor generates waste at production sites and then commissions carrier to transport it and pays accordingly. The carrier's recycling plan significantly impacts the environment, influenced by transport modes and recycling methods. Diesel trucks are cheaper but more polluting, while electric trucks are cleaner but more costly, making carriers favor diesel trucks without government subsidies. Recycling methods also vary in environmental impact; some waste can be sent directly to backfill sites, while others require harmless treatment at facilities before recycling (Chu et al., 2012). The processing facilities differ in pollutant outputs due to technological limitations. Carriers often prioritize convenience by selecting the nearest facilities, regardless of environmental concerns.

The core of the recycling plan lies in scheduling truck movements among different sites. While most existing studies concentrate on CW generation, assessment, and macro-level management (Lu et al., 2017; Gálvez-Martos et al., 2018; Trivedi et al., 2023), relatively few have focused on optimizing detailed transportation scheduling. For example, Chu et al. (2012) improved transportation efficiency by modeling the spatiotemporal flow of trucks and CW using a multi-commodity network flow model. Yazdani et al. (2021) considered travel time uncertainty and proposed a hybrid genetic algorithm to optimize vehicle routing. Chen et al. (2024) incorporated pollution from transportation and processing into a mixed-integer bi-level programming model.

Though existing studies offer valuable insights into model formulation and algorithmic design, several critical gaps in research remain. First, due to space constraints at operational sites, truck queuing and congestion are common in practice but rarely accounted for in existing models, limiting their applicability. Second, the government's goal of minimizing pollution often conflicts with the carrier's goal of profit, yet few studies have explored how the government intervenes in the decision-making of the carrier. Overall, a unified modeling framework that jointly considers transportation efficiency, environmental sustainability, and economic incentives is still lacking.

This study aims to bridge these gaps by developing an economic, efficient and environmentally friendly scheduling method that incorporates the government's indirect influence through subsidies. Penalties are not considered, as they can lead to irregularities, potentially worsening safety and pollution issues (Beliën et al., 2014).

The main contributions of this paper are as follows.

1) To enhance transportation efficiency, we formulate a tailored multi-vehicle minimum-cost flow model on a time-space network that optimizes the carrier's recycling plan and maximize profit. The model improves solution efficiency by representing site congestion through service arcs, effectively modeling queues. Results from a large instance show that the model can be solved by commercial solver within a short time.

2) To reduce environmental pollution and government expenditure on subsidizing the transportation and processing of CW, this study formulates a bi-level optimization model, with the government as the leader and the carrier as the follower. The lower-level model is a multi-vehicle minimum-cost flow model, while the upper-level model minimizes environmental pollution by optimizing To reduce environmental pollution and government expenditure on subsidizing the transportation and processing of CW, this study formulates a bi-level optimization model, with the government as the leader and the carrier as

the follower. The lower-level model is a multi-vehicle minimum-cost flow model, while the upper-level model minimizes environmental pollution by optimizing government subsidies.

3) We develop an effective hybrid heuristic algorithm to solve the complex bi-level optimization model. The algorithm employs multi-objective particle swarm optimization (MOPSO) to explore solutions for the upper-level problem, while iteratively solving the lower-level problem to refine the best local optimum. It achieves a high-quality solution with a 1.51% gap in a reasonable time of 3.76 hours.

2. Literature review

Dealing with CW is a global problem that requires a concerted effort from multiple entities. Section 2.1 reviews the CW recycling process from a management perspective. Section 2.2 reviews studies that impose economic levers on CW management and presents research gaps.

2.1. CW management scheme

The framework of CW management can be divided into four stages: pre-construction, construction, transportation, and disposal (Gálvez-Martos et al., 2018). At the pre-construction stage, carriers need to prepare plans under the supervision of the government, such as estimating waste production, evaluating environmental impacts, and developing operational plans as well as economic drivers such as subsidies, fines, and taxes. During construction, the main considerations are reducing waste, reusing materials, storage, and sorting. The transportation process is quite important yet difficult to schedule. This stage is concerned with transportation efficiency, traffic safety, environmental pollution, etc. The disposal stage is mainly responsible for the harmless treatment of CW. The authorities set strict regulations to avoid illegal disposal (Chen et al., 2024).

Estimating the volume of CW is a prerequisite for developing a transport plan. CW production estimation is widely studied in construction waste management and can be categorized into three methods: site visits (SV), generation rate calculation (GRC), and classification system accumulation (CSA) (Lu et al., 2017). The choice of method depends on the specific objectives and conditions. SV involves field surveys, which are realistic but costly and difficult to replicate. GRC, the most common method, estimates CW based on waste generation rates for specific activities or companies. It is simple and cost-effective, but less accurate. CSA is more detailed, quantifying different types of CW, and offers more reliable data at a lower cost. Studies like Solís-Guzmán et al. (2009) and Llatas (2011) applied CSA for more precise estimation, though some models are region-specific. Guerra et al. (2020) combined 4D-BIM for estimating concrete and waste. CSA provides effective, low-cost information for various CW types, forming a solid foundation for optimizing construction processes and waste management.

Transportation of CW is one of the most important and expensive processes in groundwork due to the high volume of waste, time-sensitive production rate and processing cost, and demand for heavy trucks (Aringhieri et al., 2018). Heavy trucks will affect the traffic operation of ordinary vehicles, inducing traffic congestion as well as serious accidents (Wang et al., 2022a). They also account for a large proportion of emissions which therefore poses a great challenge to the carbon neutral and pollution reduction efforts (Wijnsma et al., 2023). The complexity of the transportation networks and designs can lead to inefficient transportation.

Over the past decades, extensive research has been conducted on the transportation of various types of waste (Wang et al., 2020, 2022b). However, studies specifically focusing on the optimization of CW transportation remain relatively limited and vary in scope. Among

a few related studies, Chu et al. (2012) aimed to maximize carrier profit by modeling the spatiotemporal flow of trucks and CW as a multi-commodity network flow problem, and employed a genetic algorithm to improve transportation efficiency. Yazdani et al. (2021) brought the uncertainty of travel times into the model and developed a simulation-based optimization approach using a genetic algorithm to optimize vehicle routing. Similarly, Yi et al. (2024) incorporated the uncertainty of CW generation and formulated an integer programming model based on stochastic programming to optimize transportation plans. There are also a couple of studies focusing on the empirical aspect of this problem. For example, based on a real-world case in Hong Kong, Bi et al. (2022) identified three critical issues in CW transportation: suboptimal facility selection, disordered trip chains, and significant underloading. To address these challenges, the authors constructed an order-to-order distance matrix and proposed a combined optimization strategy that simultaneously improved (1) facility selection, (2) order sequencing, and (3) vehicle loading rates. Their results demonstrated that the integrated strategy achieved the best performance, with facility selection contributing most significantly to the improvement. However, most studies have focused on operational efficiency and ignored environmental issues.

2.2. Economic leverage for CW management scheme

Economic leverage is a key method to influence carriers in waste transportation (Wang et al., 2023, 2024). The EU introduced waste disposal charges in 1999, with fees for inert materials like concrete and tiles set at 53 euros per cubic meter, while hazardous chemicals cost 86 euros (Li et al., 2018). In Hong Kong, a waste disposal charge scheme has been in place since 2006. A study by Hao et al. (2008) found that the scheme effectively reduced waste production. Research on carriers' willingness to pay for treatment fees shows that while it exceeds current rates, it is still lower than the government's expectations(Li et al., 2020). Chen et al. (2024) suggested that many charging policies focus more on improving transport efficiency than reducing pollution, and that Hong Kong's program may have limited long-term impact. Meanwhile, Elshaboury et al. (2022) noted that policies in China to reduce waste and promote recycling have had little effect.

Compared to the evaluation of construction waste treatment fees, relatively fewer studies have focused on the design of pricing and incentive mechanisms. Under normal operating conditions, governments often prefer incentive schemes over penalties, as punitive measures may induce non-compliance and lead to more severe pollution and safety issues (Beliën et al., 2014; Wijnsma et al., 2023). Yuan and Wang (2014) pointed out that most regions in China adopt empirically determined treatment fees, which have shown limited effectiveness. To address this, they were among the first to employ system dynamics to simulate different policy scenarios and identify reasonable fee structures. Building on this, Jia et al. (2017) further explored the effects of treatment fees on illegal dumping, recycling, and reuse, and proposed an improved system dynamics method to determine an effective fee range. Alternatively, Zheng et al. (2024) developed a differential game model to examine how government subsidies and consumers' green preferences influence firms' decisions and recycling rates, providing valuable insights for the design of effective incentives and regulatory strategies. Going a step further, Chen et al. (2024) proposed a treatment fee design method that incorporates carrier behavior and external transportation impacts. A mixed-integer programming model was formulated to revise existing fee structures and better align with environmental protection goals.

In summary, although existing studies have made important progress in model development and policy design, the following problems remain unaddressed: (1) Most studies fail to simultaneously consider the coordination among multiple trucks, multiple sites, and their service capacities. As a result, truck queuing and congestion within sites are often overlooked,

leading to suboptimal transportation plans; (2) Some studies focus solely on carrier-side objectives and neglect pollution emissions generated during transportation and processing; (3) Many rely on system dynamics approaches to evaluate disposal fee policies from a macro perspective, which limits their ability to capture the strategic interactions among different decision-makers. To address these gaps, we first develop a time-space network-based multi-vehicle minimum-cost flow model to optimize the carrier's recycling schedule. Building on this, we propose a bi-level optimization model based on the Stackelberg game framework. By designing differentiated disposal fee schemes, the model guides carriers toward more environmentally sustainable decisions and provides theoretical support for the government to develop refined incentive policies.

The following texts of this paper are organized as follows. Section 3 introduces the movements of the trucks among different types of sites and formulates the mathematical models. Section 4 designs a solution algorithm and evaluation metrics. The case study and conclusions are presented in Sections 5 and 6, respectively.

3. Mathematical formulations

This section begins by outlining the assumptions and setting of the research problem. Next, the time-space network for truck movements is introduced, which serves as the foundation for the carrier's problem, i.e., the lower-level model. Finally, the upper-level problem, formulated as a liner programming model, aims to optimize the government's strategy by minimizing both pollution and subsidy expenditure. The complete bi-level problem is presented at the end.

3.1. Problem statement

We develop a bi-level optimization model inspired by the Stackelberg game, where the government acts as the leader and the carrier as the follower. The government aims to minimize pollution and subsidy expenditure, while the carrier focuses on maximizing profit. Specifically, when a carrier transports CW to processing facilities, it is required to pay treatment fees. To influence carriers' transportation decisions, the government may provide subsidies for specific types of trucks (e.g., those that generate lower emissions during transportation) and for processing facilities (e.g., those that can help reduce pollution). In turn, these transportation decisions affect both pollution levels and government subsidies. The structure of the bi-level model is illustrated in Fig. 1, and all parameters and variables are defined in Appendix A.

[Figure 1 near here]

We consider both the E electrical fleets $\mathcal{F}_e = \{\mathcal{V}_1, ..., \mathcal{V}_E\}$ and $\overline{D}$ diesel fleets $\mathcal{F}_d = \{\mathcal{V}_{E+1}, ..., \mathcal{V}_{E+\overline{D}}\}$, where the number of truck in each fleet $v \in \mathcal{F}_e \cup \mathcal{F}_d$ is represented N_v. Due to policy constraints, each truck is operated by a dedicated driver and runs for only one planning period before taking a mandatory rest. Since the battery range of electric trucks exceeds a single planning period, recharging is not a concern. Moreover, as trucks operate in a full-load mode between designated loading and unloading sites, the problem differs substantially from traditional vehicle routing problems in both structure and characteristics.

Consequently, we develop the truck movements across different sites and periods as flows in a time-space network $\mathcal{G} = \{\mathcal{N}, \mathcal{A}\}$, where $\mathcal{N}$ is a set of nodes and $\mathcal{A}$ is a set of directed arcs on the network as shown in Fig. 2. Node set includes three types within the system: processing facilities $\mathcal{P} = \{1, ..., P\}$, production sites $\mathcal{S} = \{P+1, ..., P+S\}$, and backfill sites $\mathcal{D} = \{P+S+1, ..., P+S+D\}$, with the total number is S, P, and D respectively. We consider one depot, represented as the set $\{0\}$. The planning period $\mathcal{T} = \{0, 1, ..., T\}$, where T represents the number of time intervals, Δt represents time interval. To facilitate the mathematical formulation of the model, we define the virtual planning period $\overline{\mathcal{T}} = \{-1, ..., -\overline{T}\}$, where $\overline{T}$ is a given integer. Each node $n_{i,t} \in \mathcal{N}$ represents site $i \in \{0\} \cup \mathcal{P} \cup \mathcal{S} \cup \mathcal{D}$ in period $t \in \mathcal{T} \cup \overline{\mathcal{T}}$. We

assume that truck take $r_{i,j}$ time intervals to travel from area i to area j for $i, j \in \{0\} \cup \mathcal{P} \cup \mathcal{S} \cup \mathcal{D}$. The flow on the directed arc $(n_{i,t-r_{i,j}}, n_{j,t}) \in \mathcal{A}$ represents the number of truck moving from node $n_{i,t-r_{i,j}}$ to node $n_{j,t}$ for $i, j \in \{0\} \cup \mathcal{P} \cup \mathcal{S} \cup \mathcal{D}$ and $t \in \mathcal{T} \cup \overline{\mathcal{T}}$. Based on the real-world situation, we categorize the truck movements between two nodes into three categories, i.e., *fully loaded arcs*, *deadheading arcs*, and *service arcs*. They are defined as follows.

[Figure 2 near here]

Definition 1 (Fully loaded arc). *A fully loaded arc $(n_{i,t-r_{i,j}}, n_{j,t}) \in \mathcal{A}^f$ represents the trip that trucks loaded with waste at node $n_{i,t-r_{i,j}}$ move to node $n_{j,t}$ to get unloaded, $t \in \mathcal{T}$, $i, j \in \{0\} \cup \mathcal{P} \cup \mathcal{S} \cup \mathcal{D}$.*

Specifically, fully loaded arcs include three categories depending on the conditions i, j: 1) $i \in \mathcal{S}, j \in \mathcal{D}$, trucks transport waste from production sites to backfill sites; 2) $i \in \mathcal{S}, j \in \mathcal{P}$, trucks transport waste from production sites to processing facilities for harmless treatment or storage, etc; 3) $i \in \mathcal{P}, j \in \mathcal{D}$, when waste generated from production sites is not sufficient to meet the needs of backfill sites, trucks will transport waste from processing facilities to backfill sites for pit filling.

Definition 2 (Deadheading arc). *A deadheading arc $(n_{i,t-r_{i,j}}, n_{j,t}) \in \mathcal{A}^d$ represents the trip in which trucks travel from node $n_{i,t-r_{i,j}}$ to node $n_{j,t}$ in empty, $t \in \mathcal{T}$, $i, j \in \{0\} \cup \mathcal{P} \cup \mathcal{S} \cup \mathcal{D}$.*

Specifically, deadheading arcs include four categories depending on the conditions i, j: 1) $i \in \{0\}, j \in \mathcal{P} \cup \mathcal{S}$, at the beginning of the planning period, the trucks travel from the depot to production sites or processing facilities to load waste; 2) $i \in \mathcal{P} \cup \mathcal{D}, j \in \{0\}$, at the end of the planning period, trucks travel from backfill sites or processing facilities to the depot for rest; 3) $i \in \mathcal{D}, j \in \mathcal{P} \cup \mathcal{S}$, trucks travel to production sites or processing facilities to load waste after unloading at backfill sites; 4) $i \in \mathcal{P}, j \in \mathcal{S}$, similar to above, trucks travel to production sites to load waste after unloading at processing facilities.

Definition 3 (Service arc). *A service arc $(n_{i,t_1}, n_{i,t_2}) \in \mathcal{A}^s$ represents the waiting phase in which trucks arrive at node n_{i,t_1} and then moves to node n_{i,t_2}, $i \in \{0\} \cup \mathcal{P} \cup \mathcal{S} \cup \mathcal{D}$, $t_1, t_2 \in \mathcal{T}$. In other words, the trucks stay at site i for one time intervals Δt.*

Upon arrival, trucks queue, load (or unload), check, clean, and then depart. The total service time depends on the site's capacity. For simplicity, we assume the service time is a time interval Δt, which is typically longer than the actual service time, providing a buffer for travel and delays. Similar assumptions are used in transportation planning (Carey and McCartney, 2003). Thus, the service arc $(n_{i,t-1}, n_{i,t}) \in \mathcal{A}^s$ represents the waiting phase where trucks arrive at node $n_{i,t-1}$, stay for Δt, and then depart from node $n_{i,t}$, with $i \in \mathcal{P} \cup \mathcal{S} \cup \mathcal{D}$ and $t \in \mathcal{T}$.

Except for the three types of arcs mentioned, all other arcs in $\mathcal{A}$ have a flow of 0, represented as the set $\mathcal{A}^0$. We define $\mathcal{I} = \{f, d, s, 0\}$, so that $\mathcal{A} = \cup_{\forall e \in \mathcal{I}} \mathcal{A}^e$ and $\mathcal{A}^{e_1} \cap \mathcal{A}^{e_2} = \emptyset$ for $e_1 \neq e_2, e_1, e_2 \in \mathcal{I}$. We then formulate an integer programming problem based on the time-space network in Fig. 2 to maximize the carrier's profit.

3.2. The strategy of the carrier

In this section, we formulate a model based on the time-space network $\mathcal{G}$ to maximize the carrier's profit (or equivalently, minimize the negative of the carrier's profit), with three components: 1) Fixed cost, where $C_{0,v}$ is the fixed cost per truck in fleet $v \in \mathcal{F}_e \cup \mathcal{F}_d$, covering the driver's salary, truck maintenance, etc. (Beliën et al., 2014). 2) Travel cost, where $C_{1,v}$ is the average cost per truck in fleet v for traveling one time interval Δt, mainly covering fuel or electricity costs. 3) Revenue from waste transport, with a unit price of C_2 CNY per tonne.

However, if the waste is sent to processing facilities, the carrier incurs an additional treatment fee, which is either a fixed market price y' or a variable fee, discussed in Section 3.3.2. The task volume for each planning period is known in advance, and CW accumulation costs on-site are excluded.

We define decision variable $x_{i,j,v,t}$ as the flow of fleet $v \in \mathcal{F}_e \cup \mathcal{F}_d$ from node $n_{i,t} \in \mathcal{N}$ to another node $n_{j,t+r_{i,j}} \in \mathcal{N}$ at time $t \in \mathcal{T} \cup \overline{\mathcal{T}}$. All of the notations are shown in Appendix A, and the mathematical model is as follows:

[M1]

$$\text{Min } f(\mathbf{x}) = \overbrace{\sum_{v\in\mathcal{F}_e\cup\mathcal{F}_d}\sum_{j\in\mathcal{P}\cup\mathcal{S}\cup\mathcal{D}}\sum_{t\in\mathcal{T}} C_{0,v}x_{0,j,v,t}}^{\text{fixed cost}} + \overbrace{\sum_{v\in\mathcal{F}_e\cup\mathcal{F}_d}\sum_{i\in\mathcal{P}\cup\mathcal{S}\cup\mathcal{D}}\sum_{j\in\mathcal{P}\cup\mathcal{S}\cup\mathcal{D}}\sum_{t\in\mathcal{T}} C_{1,v}r_{i,j}x_{i,j,v,t}}^{\text{travel cost}} - \overbrace{(\sum_{v\in\mathcal{F}_e\cup\mathcal{F}_d}\sum_{i\in\mathcal{S}\cup\mathcal{P}}\sum_{j\in\mathcal{D}}\sum_{t\in\mathcal{T}} C_2Q_vx_{i,j,v,t} + \sum_{v\in\mathcal{F}_e\cup\mathcal{F}_d}\sum_{i\in\mathcal{S}}\sum_{j\in\mathcal{P}}\sum_{t\in\mathcal{T}}(C_2-y')Q_vx_{i,j,v,t})/1,000}^{\text{revenue from transporting CW}}; \tag{1}$$

Subject to:

$$\sum_{j\in\mathcal{P}\cup\mathcal{S}\cup\mathcal{D}}\sum_{t\in\mathcal{T}} x_{0,j,v,t} \le N_v, \forall v \in \mathcal{F}_e \cup \mathcal{F}_d; \tag{2}$$

$$\sum_{j\in\mathcal{P}\cup\mathcal{S}\cup\mathcal{D}}\sum_{t\in\mathcal{T}} x_{0,j,v,t} - \sum_{i\in\mathcal{P}\cup\mathcal{S}\cup\mathcal{D}}\sum_{t\in\mathcal{T}} x_{i,0,v,t} = 0, \forall v \in \mathcal{F}_e \cup \mathcal{F}_d; \tag{3}$$

$$\sum_{i\in\{0\}\cup\mathcal{P}\cup\mathcal{S}\cup\mathcal{D}} x_{i,j,v,t-r_{i,j}-1} - \sum_{i\in\{0\}\cup\mathcal{P}\cup\mathcal{S}\cup\mathcal{D}} x_{j,i,v,t} = 0, \forall j \in \mathcal{P}\cup\mathcal{S}\cup\mathcal{D}, \forall v \in \mathcal{F}_e\cup\mathcal{F}_d, \forall t \in \mathcal{T}; \tag{4}$$

$$\sum_{i\in\{0\}\cup\mathcal{P}\cup\mathcal{S}\cup\mathcal{D}}\sum_{v\in\mathcal{F}_e\cup\mathcal{F}_d} x_{i,j,v,t-r_{i,j}} \le B_j, \forall j \in \mathcal{P}\cup\mathcal{S}\cup\mathcal{D}, \forall t \in \mathcal{T}; \tag{5}$$

$$\sum_{j\in\mathcal{P}\cup\mathcal{D}}\sum_{v\in\mathcal{F}_e\cup\mathcal{F}_d}\sum_{t\in\mathcal{T}} Q_vx_{i,j,v,t}/1,000 = qs_i, \forall i \in \mathcal{S}; \tag{6}$$

$$\sum_{i\in\mathcal{P}\cup\mathcal{S}}\sum_{v\in\mathcal{F}_e\cup\mathcal{F}_d}\sum_{t\in\mathcal{T}} Q_vx_{i,j,v,t}/1,000 = qd_j, \forall j \in \mathcal{D}; \tag{7}$$

$$x_{i,j,v,t} = 0, \forall i \in \{0\}\cup\mathcal{P}\cup\mathcal{S}\cup\mathcal{D}, \forall j \in \{0\}\cup\mathcal{P}\cup\mathcal{S}\cup\mathcal{D}, \forall v \in \mathcal{F}_e\cup\mathcal{F}_d, \forall t \in \overline{\mathcal{T}}; \tag{8}$$

$$x_{i,j,v,t} = 0, \exists\mathcal{H} \in \{\{0\},\mathcal{P},\mathcal{S},\mathcal{D}\}, \forall i,j \in \mathcal{H}, \forall v \in \mathcal{F}_e\cup\mathcal{F}_d, \forall t \in \mathcal{T}; \tag{9}$$

$$x_{i,j,v,t} \in \{0,1,...,B_j\}, \forall i,j \in \{0\}\cup\mathcal{P}\cup S\cup D, \forall v \in \mathcal{F}_e\cup\mathcal{F}_d, \forall t \in \mathcal{T}\cup\overline{\mathcal{T}}. \tag{10}$$

Constraint (2) ensures that the total number of trucks traveling from the depot to the sites is less than the total number of trucks in the fleet. Constraint (3) ensures that the number of trucks traveling from the depot equals the number of trucks returning to the depot. Constraint (4) indicates that the node flow is conserved. Constraint (5) restricts the maximum number of trucks arriving at a site simultaneously to avoid congestion. Constraint (6) ensures that the CW generated from each production site is fully transported. Constraint (7) ensures that the needs of each backfill site are satisfied. Constraints (8) and (9) filter infeasible transport arcs. Constraint (10) is an integer constraint that the upper flow limit should be

equal to the operating capacity of the operating area. Solving the model [**M1**] generates an efficient scheduling for the carrier.

3.3. The strategy of the government

The profit objective for subsidizing is straightforward. We first demonstrate how the pollution related objective is computed in Section 3.3.1 and present the full bi-level model in Section 3.3.2.

3.3.1. Calculate method of pollution

Pollution from CW transportation consists of two components: emissions from diesel trucks during transportation and pollution from waste treatment at processing facilities. To improve realism, truck emissions are typically estimated using the Comprehensive Modal Emissions Model (CMEM) (Demir et al., 2014). Based on this model, the Fuel Consumption Rate (FCR) is given by:

$$FCR = \frac{\xi(kNV + P_0/\eta)}{\kappa}, \tag{11}$$

where ξ is the fuel-to-air mass ratio, k is the engine friction factor, N and V denote the engine speed and engine displacement, respectively. The parameters η and κ are constants representing efficiency and the heating value, respectively. P_0 is the second-by-second engine power output (in kilowatts) and can be calculated as:

$$P_0 = \frac{P_t}{\eta_t} + P_a, \tag{12}$$

where η_t denotes the truck drive train efficiency, and P_a is the engine power requirement associated with the operating losses of the engine and the operation of truck accessories (e.g., air conditioning). P_a is typically assumed to be 0 (Demir et al., 2011). P_t represents the total traction force, which is the force generated by the friction between the truck tires and the road surface. P_t can be calculated as follows:

$$P_t = \frac{(M_v\tau + M_v g sin\delta + 0.5 f_a \varphi A u + M_v g f_r cos\delta)u}{1,000}, \tag{13}$$

where M_v is the truck's total weight in feet $v \in \mathcal{F}_e \cup \mathcal{F}_d$, including both the unloaded weight ($\overline{Q}_v$) and rated load (Q_v). τ is acceleration, g is gravitational acceleration, and δ is the road angle. The coefficients f_a and f_r represent aerodynamic drag and rolling resistance, respectively. φ is air density, and A is the truck's frontal area. u is the truck's speed. For simplicity, Demir et al. (2014) defines $\lambda = \frac{\xi}{\kappa\theta}$, $\gamma = \frac{1}{1{,}000\eta_t\eta}$, $\alpha = \tau + g\sin\delta + gf_r\cos\delta$, and $\beta = 0.5 f_d \varphi A$, where θ is the fuel conversion factor from $\frac{gram}{s}$ to $\frac{liter}{s}$, and ξ is typically assumed to be 1 (Demir et al., 2011). Thus, the pollution value (Fuel Consumption, FC) for a diesel truck $v \in \mathcal{F}_d$ over a distance d is a function of speed u and total weight $M = \overline{Q}_v + Q_v$:

$$FC(u, M) = \frac{\lambda(kNV + \overline{Q}_v\gamma\alpha u + Q_v\gamma\alpha u + \beta\gamma u^3)d}{u}, \forall v \in \mathcal{F}_d. \tag{14}$$

Pollution from processing facilities primarily depends on the facility's capacity and the volume of CW processed. The pollution generated by the harmless treatment of one tonne of CW at a facility $j \in \mathcal{P}$ is defined by the pollution factor h_j. Therefore, the pollution value for processing a truckload of CW from fleet $v \in \mathcal{F}_e \cup \mathcal{F}_d$ at facility $j \in \mathcal{P}$ is expressed as:

$$HTC = h_j Q_v, \forall j \in \mathcal{P}, \forall v \in \mathcal{F}_e \cup \mathcal{F}_d. \tag{15}$$

3.3.2. Mathematical formulation

The objective of the upper-level problem is to minimize pollution induced by CW transport and processing while minimizing the government subsidies. The compound objective function could be derived from (14) and (15). The lower-level problem corresponds to [**M1**]. The decision variables for the upper-level problem are $y_{j,v}$s, representing the treatment fees for the harmless treatment per ton of CW carried by fleet $v \in \mathcal{F}_e \cup \mathcal{F}_d$ at processing facility $j \in \mathcal{P}$. They form input parameters to the lower-level problem. The decision variable for the lower-level problem is $x_{i,j,v,t}$, and the optimal solution for the lower-level problem is denoted by $x'_{i,j,v,t}$, $i, j \in \{0\} \cup \mathcal{P} \cup S \cup D, v \in \mathcal{F}_e \cup \mathcal{F}_d, t \in \mathcal{T} \cup \overline{\mathcal{T}}$. The bi-level program is given by:

[M2]

$$\begin{aligned}\text{Min } F_1(\mathbf{x}'|\mathbf{y}) = & \sum_{i\in\mathcal{P}\cup\mathcal{S}\cup\mathcal{D}}\sum_{j\in\mathcal{P}\cup\mathcal{S}\cup\mathcal{D}}\sum_{v\in\mathcal{F}_d}\sum_{t\in\mathcal{T}} kNV\lambda d_{i,j}x'_{i,j,v,t}/u \\ & + \sum_{i\in\mathcal{P}\cup\mathcal{S}\cup\mathcal{D}}\sum_{j\in\mathcal{P}\cup\mathcal{S}\cup\mathcal{D}}\sum_{v\in\mathcal{F}_d}\sum_{t\in\mathcal{T}} \overline{Q}_v\gamma\lambda\alpha_{i,j}d_{i,j}x'_{i,j,v,t} \\ & + (\sum_{i\in\mathcal{S}}\sum_{j\in\mathcal{P}\cup\mathcal{D}}\sum_{v\in\mathcal{F}_d}\sum_{t\in\mathcal{T}} Q_v\gamma\lambda\alpha_{i,j}d_{i,j}x'_{i,j,v,t} + \sum_{i\in\mathcal{P}}\sum_{j\in\mathcal{D}}\sum_{v\in\mathcal{F}_d}\sum_{t\in\mathcal{T}} Q_v\gamma\lambda\alpha_{i,j}d_{i,j}x'_{i,j,v,t}) \\ & + \sum_{i\in\mathcal{P}\cup\mathcal{S}\cup\mathcal{D}}\sum_{j\in\mathcal{P}\cup\mathcal{S}\cup\mathcal{D}}\sum_{v\in\mathcal{F}_d}\sum_{t\in\mathcal{T}} \beta\gamma\lambda d_{i,j}x'_{i,j,v,t}u^2 \\ & + \sum_{i\in\mathcal{S}}\sum_{j\in\mathcal{P}}\sum_{v\in\mathcal{F}_e\cup\mathcal{F}_d}\sum_{t\in\mathcal{T}} h_jQ_vx'_{i,j,v,t};\end{aligned} \tag{16}$$

Subject to:

$$y_{j,v} \geq PL, \forall j \in \mathcal{P}, \forall v \in \mathcal{F}_e \cup \mathcal{F}_d; \tag{17}$$

$$y_{j,v} \leq PU, \forall j \in \mathcal{P}, \forall v \in \mathcal{F}_e \cup \mathcal{F}_d; \tag{18}$$

where

$$\begin{aligned}\mathbf{x}' \in \arg\min\{f'(\mathbf{x},\mathbf{y}) = & \sum_{v\in\mathcal{F}_e\cup\mathcal{F}_d}\sum_{j\in\mathcal{P}\cup\mathcal{S}\cup D}\sum_{t\in\mathcal{T}} C_{0,v}x_{0,j,v,t} \\ & + \sum_{v\in\mathcal{F}_e\cup\mathcal{F}_d}\sum_{i\in\mathcal{P}\cup\mathcal{S}\cup\mathcal{D}}\sum_{j\in\mathcal{P}\cup\mathcal{S}\cup\mathcal{D}}\sum_{t\in\mathcal{T}} C_{1,v}r_{i,j}x_{i,j,v,t} \\ & - \sum_{v\in\mathcal{F}_e\cup\mathcal{F}_d}\sum_{i\in\mathcal{S}\cup\mathcal{P}}\sum_{j\in\mathcal{D}}\sum_{t\in\mathcal{T}} C_2Q_vx_{i,j,v,t} \\ & - \sum_{v\in\mathcal{F}_e\cup\mathcal{F}_d}\sum_{i\in\mathcal{S}}\sum_{j\in\mathcal{P}}\sum_{t\in\mathcal{T}}(C_2 - y_{j,v})Q_vx_{i,j,v,t}\};\end{aligned} \tag{19}$$

Subject to:

Constraints (2)-(10).

Constraint (17) limits the treatment fees to the government's budget, with PL representing the minimum acceptable price. Constraint (18) sets the maximum price, PU, acceptable to the carrier; exceeding this may lead to illegal shipment or processing risks (Beliën et al., 2014). Constraint (19) minimizes the negative of the carrier's profit (i.e., maximize the carrier's profit), derived from function (1) by replacing y' with the variable $y_{j,v}, j \in \mathcal{P}, v \in \mathcal{F}_e \cup \mathcal{F}_d$. Model [**M2**] has the following property:

Property 1. *As government subsidies increase, the objective of model* [**M2**] *is non-increasing.*

Property 2. *The objective of* [**M2**] *has a natural lower bound, e.g., pollution will not be less than 0.*

The proofs are omitted because they are straightforward. Property 1 shows that the government can reduce pollution by increasing the subsidy investment. However, Property 2 indicates that beyond a certain subsidy level, further increases do not result in additional pollution reduction, leading to multiple optimal solutions for [**M2**]. Since the government aims to minimize pollution with the least subsidy investment, we introduce the second objective function to minimize subsidies. We assume that $x^{M1}_{i,j,v,t}$s are the optimal solution of the model **[M1]**, the government subsidies (GS) is calculated as follows:

$$GS = \sum_{i\in\mathcal{S}}\sum_{j\in\mathcal{P}}\sum_{v\in\mathcal{F}_e\cup\mathcal{F}_d}\sum_{t\in\mathcal{T}} y' Q_v x^{M1}_{i,j,v,t} - \sum_{i\in\mathcal{S}}\sum_{j\in\mathcal{P}}\sum_{v\in\mathcal{F}_e\cup\mathcal{F}_d}\sum_{t\in\mathcal{T}} y_{j,v} Q_v x_{i,j,v,t} \tag{20}$$

where $\sum_{i\in\mathcal{S}}\sum_{j\in\mathcal{P}}\sum_{v\in\mathcal{F}_e\cup\mathcal{F}_d}\sum_{t\in\mathcal{T}} y' Q_v x^{M1}_{i,j,v,t}$ represents the origin total treatment fees without subsidies, while $\sum_{i\in\mathcal{S}}\sum_{j\in\mathcal{P}}\sum_{v\in\mathcal{F}_e\cup\mathcal{F}_d}\sum_{t\in\mathcal{T}} y_{j,v} Q_v x_{i,j,v,t}$ represents the actual total treatment fees paid by the carrier under the subsidy scheme. Since y', Q_v ($v \in \mathcal{F}_d$), and the waste volume $\sum_{i\in\mathcal{S}}\sum_{j\in\mathcal{P}}\sum_{v\in\mathcal{F}_e\cup\mathcal{F}_d}\sum_{t\in\mathcal{T}} x^{M1}_{i,j,v,t}$ are constants, the former term remains constant. Therefore, when implementing subsidy scheme, government subsidies are a linear function of the carrier's actual total treatment fees (hereafter referred to as total treatment fees), with a slope of -1.

To simplify the mathematical formulation, we directly minimize the negative of the total treatment fees, which is equivalent to minimizing government subsidies. Accordingly, the bi-level model is formulated as follows:

[M3]

$$\text{Min } F_2(\mathbf{x},\mathbf{y}) = -\sum_{i\in\mathcal{S}}\sum_{j\in\mathcal{P}}\sum_{v\in\mathcal{F}_e\cup\mathcal{F}_d}\sum_{t\in\mathcal{T}} y_{j,v} Q_v x'_{i,j,v,t}; \tag{21}$$

Subject to:

$$F_1(\mathbf{x}'|\mathbf{y}) = F_1(\mathbf{x}^*_{M2}); \tag{22}$$

Constraints (17) – (18);

where

$$\mathbf{x}' \in \arg\min\{f'(\mathbf{x},\mathbf{y})\}; \tag{23}$$

Subject to:

Constraints (2)-(10).

The objective function (21) minimizes the negative of total treatment fees (i.e., minimizes the government subsidies). The function F_1 in constraint (22) is derived from objective function (16), where $\mathbf{x}^*_{M2}$ represents the optimal solution of $\mathbf{x}^*$ acquired by solving **[M2]**, and $F_1(\mathbf{x}^*_{M2})$ is optimal value for **[M2]**. Therefore, constraint (22) ensures that the total pollution must be minimized. Constraint (23) is identical to constraint (19). Solving model **[M3]** yields the economical and environmentally friendly scheduling.

Remark 1. *Model [M3] could also be formulated as a tri-level optimization model, where the upper level optimizing government subsidies, the middle level minimizing total pollution, and the lower level maximizing the carrier's profit. However, this interpretation will complicate the model structure and lead to sub-optimal solutions. Instead, we formulate it as a bi-level model, where the upper level includes a primary objective F_1 (total pollution) and a secondary objective F_2 (the opposite of the total treatment fees).*

4. Solution approach

Section 4.1 outlines a hybrid approach to address the bi-level optimization model **[M3]**. The method for calculating the model gap is detailed in Section 4.2.

4.1. Solution algorithm

Standard minimum-cost flow models typically possess a totally unimodular constraint matrix, ensuring that their linear relaxations yield integer optimal solutions (Ahuja et al., 1993). Although our model **[M1]** does not strictly exhibit this property, its linear relaxation still produces solutions that are very close to integer optima. As a result, high-quality solutions can be efficiently obtained using commercial solvers. Model **[M2]** serves as an intermediate formulation in the derivation process and does not require independent solving. Model **[M3]** is a bi-level optimization problem, where the upper level is a linear program and the lower level is a relatively large-scale integer program, making exact solution computationally difficult. While iterative approaches between levels have been proposed in prior studies (Soares et al., 2021), our preliminary experiments reveal that such methods often require additional constraints on the lower-level problem to ensure convergence. These modifications disrupt the original network flow structure, rendering commercial solvers less effective. Given that particle swarm optimization is particularly suitable for problems with linear upper-level structures and offers advantages in convergence speed and solution stability (Sinha et al., 2017; Soares et al., 2020; Coello et al., 2004), we adopt a hybrid solution approach. Specifically, we use MOPSO to solve the upper-level problem and a commercial solver for the lower level, striking a practical balance between solution quality and computational efficiency. The algorithm flowchart as shown in Fig. 3.

[Figure 3 near here]

4.1.1. Global framework

For the model **[M1]**. Since this model involves two types of trucks with different load capacities, it is difficult to strictly satisfy constraints (6) and (7) in practical applications. Therefore, we relax these constraints into the following inequalities:

$$\sum_{j\in\mathcal{P}\cup\mathcal{D}}\sum_{v\in\mathcal{F}_e\cup\mathcal{F}_d}\sum_{t\in\mathcal{T}} Q_v x_{i,j,v,t}/1,000 \geq qs_i, \forall i \in \mathcal{S}; \tag{24}$$

$$\sum_{j\in\mathcal{P}\cup\mathcal{D}}\sum_{v\in\mathcal{F}_e\cup\mathcal{F}_d}\sum_{t\in\mathcal{T}} Q_v x_{i,j,v,t}/1,000 \leq (1+\epsilon_2) qs_i, \forall i \in \mathcal{S}; \tag{25}$$

$$\sum_{i\in\mathcal{P}\cup\mathcal{S}}\sum_{v\in\mathcal{F}_e\cup\mathcal{F}_d}\sum_{t\in\mathcal{T}} Q_v x_{i,j,v,t}/1,000 \geq qd_j, \forall j \in \mathcal{D}; \tag{26}$$

$$\sum_{i\in\mathcal{P}\cup\mathcal{S}}\sum_{v\in\mathcal{F}_e\cup\mathcal{F}_d}\sum_{t\in\mathcal{T}} Q_v x_{i,j,v,t}/1,000 \leq (1+\epsilon_2) qd_j, \forall j \in \mathcal{D}. \tag{27}$$

where ϵ_2 represents a small tolerance parameter, allowing for a slight surplus after fulfilling the demands qs and qd.

For the model **[M3]**, the hybrid approach combines a multi-objective particle swarm optimization (MOPSO) (Coello et al., 2004) to search for the solution to the upper-level problem and a commercial solver to solve the lower-level problem. We first define the total number of fleets V (i.e., $V = E + \overline{D}$). The hybrid approach begins by randomly initializing a particle swarm of K particles $\mathbf{y}^k = (y^k_{1,1}, \ldots, y^k_{1,V}, y^k_{2,1}, \ldots, y^k_{j,v}, \ldots, y^k_{P,V})$, $k = 1, \ldots, K$, representing the treatment fee set by government at processing facility $j \in \mathcal{P}$ for truck fleet $v \in \mathcal{F}_e \cup \mathcal{F}_d$. Meanwhile, randomly initialize the corresponding velocity

$\boldsymbol{\mu}^k = (\mu^k_{1,1}, \ldots, \mu^k_{1,V}, \mu^k_{2,1}, \ldots, \mu^k_{j,v}, \ldots, \mu^k_{P,V})$ of each particle $\mathbf{y}^k$. We input each $\mathbf{y}^k$ into the lower-level problem of **[M3]** to obtain a solution $\mathbf{x}^k$, where $\mathbf{x}$ represents the vector of all decision variables of the lower-level problem. The pseudocode outlines the steps of the proposed hybrid approach as follows:

Algorithm 1 Pseudocode of the Hybrid Approach

1: Initialize a particle swarm of K particles $\mathbf{y}^k = (y^k_{1,1}, \ldots, y^k_{1,V}, y^k_{2,1}, \ldots, y^k_{j,v}, \ldots, y^k_{P,V})$, velocity $\boldsymbol{\mu}^k = (\mu^k_{1,1}, \ldots, \mu^k_{1,V}, \mu^k_{2,1}, \ldots, \mu^k_{j,v}, \ldots, \mu^k_{P,V})$, $k = 1, \ldots, K$, $j \in \mathcal{P}$, $v \in \mathcal{F}_e \cup \mathcal{F}_d$
2: **repeat**
3: **for** $k = 1$ to K **do**
4: Repair $\mathbf{y}^k$ to satisfy constraints (17) and (18), retaining each $y^k_{j,v}$ to five decimal digits
5: Input $\mathbf{y}^k$ into the lower level problem and solve it using solver to obtain $\mathbf{x}^k$
6: Compute $F_1(\mathbf{x}^k)$ and $F_2(\mathbf{x}^k, \mathbf{y}^k)$ for each $(\mathbf{x}^k, \mathbf{y}^k)$
7: Update $\mathbf{y}^k$ using MOPSO (introduced in Section 4.1.2)
8: **end for**
9: **until** G iterations are completed
10: Output: $(\mathbf{x}^k, \mathbf{y}^k)$ with the best $F_1(\mathbf{x}^k)$

Line 4 of Algorithm 1 requires a repair routine that projects any $y^k_{j,v} \in \mathbf{y}^k$ to PL or PU if it violates constraint (17) or (18). The velocity of the particle is then updated by applying a negative sign, prompting the particle to search in the opposite direction. Since the treatment fee must be a fixed value in practice, even though $y^k_{j,v}$ is treated as a continuous variable in the model, it is truncated to five decimal places after initialization or updating.

4.1.2. Upper-level search based on MOPSO

The upper constraint (22) of model **[M3]** can create challenges in generating feasible solutions $\mathbf{y}^k$, $k = 1, \ldots, K$, since it represents the objective of minimizing pollution in the upper-level problem. To address this, we treat functions F_1 and F_2 as the primary and secondary objective functions, respectively. Previous experiments have shown that heuristic methods designed for single-objective optimization often focus solely on the primary objective function F_1, largely ignoring F_2. To overcome this, we initially assign equal priority to both F_1 and F_2 and use MOPSO to identify the Pareto optimal solution set. Afterward, we select the solution with the minimum value of F_1 from this set as the final high-quality solution. This approach ensures that the solution converges toward the objectives of both F_1 and F_2.

Line 6 of Algorithm 1 calculates $\mathbf{x}^k$, $\mathbf{y}^k$, $F_1(\mathbf{x}^k)$, and $F_2(\mathbf{x}^k, \mathbf{y}^k)$. Here, $\mathbf{y}^k$ is a particle in MOPSO, while $F_1(\mathbf{x}^k)$ and $F_2(\mathbf{x}^k, \mathbf{y}^k)$ represent the fitness values corresponding to the two objective functions for the current $\mathbf{x}^k$ and $\mathbf{y}^k$. MOPSO iteratively adjusts the particles to move toward optimal positions. The velocity $\boldsymbol{\mu}^k$ of each particle is influenced by both its personal best position ($\mathbf{ybest}^k$) and the position of the global best particle ($\mathbf{gbest}^k$). The global best selection mechanism follows the approach by Coello et al. (2004), with the main steps summarized as follows: (1) Define three arrays: EAY, EAF_1, and EAF_2, each of length M, to store the positions of Pareto optimal particles and their corresponding objective function values F_1 and F_2, respectively. (2) Divide the objective space into hypercubes by creating a grid with $HQ = m \times m$ cells. Each hypercube represents a region, and the particle density in each region is used to calculate its distribution. (3) Use a roulette-wheel mechanism to select a global best particle ($\mathbf{gbest}^k$) from EAY. Particles in less populated hypercubes are given higher selection probabilities, ensuring that under-explored regions are prioritized (e.g., selecting $EAY^q[i]$ at iteration q). (4) If the number of Pareto solutions exceeds the length

of EAY, particles in densely populated hypercubes are more likely to be deleted, preserving diversity in the repository. For additional technical details, refer to Coello et al. (2004).

In any iteration q, the velocity component $\mu_{j,v}^{k,q}$ of the particle $\mathbf{y}^k$ is updated according to the following equation (Kennedy and Eberhart, 1995):

$$\mu_{j,v}^{k,q} = \omega_0 \mu_{j,v}^{k,q-1} + \omega_1 R_1 (pbest_{j,v}^k - y_{j,v}^{k,q-1}) + \omega_2 R_2 (gbest_{j,v} - y_{j,v}^{k,q-1}), \tag{28}$$

where ω_0 represents the inertia weight, ω_1 and ω_2 represent cognitive and social perceptual parameters; R_1 and R_2 are random numbers uniformly distributed in the interval [0,1]; $gbest_{j,v} = EAY[i]_{j,v}, i \in \{1, \ldots, M\}$. The new position of particle $\mathbf{y}^k$ at iteration q is calculated using the following equation (Kennedy and Eberhart, 1995):

$$\mathbf{y}^{k,q} = \mathbf{y}^{k,q-1} + \boldsymbol{\mu}^{k,q}. \tag{29}$$

Particle swarm optimization converges quickly and easily falls into local optimal solutions, so we introduce random perturbations into the algorithm based on study Soares et al. (2020). If the solution does not change after $G^{'}$ iterations, the algorithm introduces perturbations with probability p_m, enhancing the exploration capability of the particles. Specifically, for each particle $\mathbf{y}^k$, after being updated by Eq. (29) and before being repaired (Line 4 in Algorithm 1), a perturbation ε is applied within the range $[-\sigma\,(PU - PL)\,, \sigma\,(PU - PL)]$, i.e., $y_{j,v}^{k,q} \leftarrow y_{j,v}^{k,q} + \varepsilon$. The algorithm terminates when the difference between objective function values from two consecutive iterations falls below a specified threshold ϵ_1, In other words, the following two inequalities are satisfied:

$$\frac{EAF_1^q[index] - EAF_1^{q-1}[index]}{EAF_1^q[index]} < \epsilon_1, \tag{30}$$

$$\frac{EAF_2^q[index] - EAF_2^{q-1}[index]}{EAF_2^q[index]} < \epsilon_1, \tag{31}$$

where $EAF_1^q[index] = \min\{EAF_1^q[1], \ldots, EAF_1^q[M]\}$, $EAF_2^q[index]$ is optimal under the condition that $EAF_1^q[index]$ is guaranteed to be optimal.

4.1.3. Accelerated lower-level problem solving

The time-space network graph $\mathcal{G}$ is a complete graph with an exponential number of edges (Fig. 2), which places a significant memory burden on the computer. However, most edges in the graph have a value of 0. For instance, a truck does not travel from sites in $\mathcal{P}$ to other sites in $\mathcal{P}$, from $\mathcal{S}$ to $\mathcal{S}$, or from $\mathcal{D}$ to $\mathcal{D}$; likewise, a production site $i \in \mathcal{S}$ only transports waste to a limited number of backfill sites $j \in \mathcal{D}$, or possibly just one. By removing these impossible edges (those with a flow rate of 0) to obtain support graph, the model size is greatly reduced. This reduction allows the commercial solver to provide an exact solution in a reasonable amount of time.

It is important to note that for each $\mathbf{y}^k$, there may be multiple possible solutions for $\mathbf{x}^k$. However, in practice, the carrier is indifferent to pollution and tends to select an $\mathbf{x}^k$ randomly (Liu et al., 2019). This randomness may lead to sub-optimal values for $F_1(\mathbf{x}^k)$ and $F_2(\mathbf{x}^k, \mathbf{y}^k)$, which can influence the MOPSO algorithm when updating the particle positions (Soares et al., 2020). Therefore, incorporating a random selection strategy can enhance the robustness of the model. Section 5.2 discusses the accuracy of the proposed method.

4.2. Optimality gap estimation and algorithmic evaluation

The upper and lower bounds of the model cannot be directly determined by the proposed hybrid approach and require further discussion. This section provides a detailed analysis of the upper and lower bounds of pollution and defines the utilization rate of government subsidies.

4.2.1. Gap of pollution value

We define $\mathbf{x}^*_{M1}$ as the optimal solution of model **[M1]**, which focuses on the carrier's profit while ignoring environmental pollution. The following proposition holds:

Proposition 1. *$F_1(\mathbf{x}^*_{M1})$ is the upper bound of the pollution value F_1 in model [M3].*

Proof. Since $\mathbf{x}^*_{M1}$ is the optimal solution of model **[M1]**, it is also a feasible solution for model **[M3]**. Therefore, $F_1(\mathbf{x}^*_{M1})$ serves as an upper bound for the pollution value in model **[M3]**. □

$F_1(\mathbf{x}^*_{M1})$ can be interpreted as the pollution generated by the carrier while transporting CW without any subsidy measures. Therefore, the rate of pollution reduction (RoPR) can be expressed as the gap between $F_1(\mathbf{x}^*_{M3})$ and $F_1(\mathbf{x}^*_{M1})$:

$$RoPR = \frac{F_1(\mathbf{x}^*_{M1}) - F_1(\mathbf{x}^*_{M3})}{F_1(\mathbf{x}^*_{M1})} \times 100\%, \tag{32}$$

where $\mathbf{x}^*_{M3}$ represents the solution obtained by solving model **[M3]** using the proposed hybrid approach. If we require $\mathbf{x}$ to be feasible rather than optimal, we can relax the bi-level model **[M2]** into a single-level model, known as the *high point problem* (Moore and Bard, 1990):

$$\begin{aligned} &\textbf{[M2-HPR]} \\ &\min F_1(\mathbf{x}) \\ &\text{subject to:} \\ &\qquad \text{Constraints (2)} - \text{(10)},\ \text{(17)},\ \text{(18)}. \end{aligned} \tag{33}$$

We define $\mathbf{x}^*_{HPR}$ represents the optimal solution of model **[M2-HPR]**. The following proposition holds:

Proposition 2. *$F_1(\mathbf{x}^*_{HPR})$ is the lower bound of F_1 in model [M3].*

Proof. $F_1(\mathbf{x}^*_{HPR})$ is the lower bound that can be interpreted from two perspectives: 1) model **[M2-HPR]** is a relaxation of model **[M2]**. 2) The objective function (33) and constraints (2)-(10) do not contain the decision variable $\mathbf{y}$, so constraints (17) and (18) can be removed from the model **[M2-HPR]**. Observing models **[M2-HPR]** and **[M1]**, we can see that they represent the truck schedule developed by the carrier and the government under the same operating conditions, respectively. □

Therefore, the GAP of the objective function F_1 in model **[M3]** is calculated as follows:

$$GAP\_F_1 = \frac{F_1(\mathbf{x}^*_{M3}) - F_1(\mathbf{x}^*_{HPR})}{F_1(\mathbf{x}^*_{HPR})} \times 100\%. \tag{34}$$

4.2.2. Effective subsidy rate of government

To reduce pollution, the carrier needs to change trucks' schedules. This will result in additional transportation costs, which should be compensated by the government. Although higher subsidies initially reduce pollution, their effect diminishes with further increases, eventually only raising the carrier's profit. The following formula measures the relationship between the carrier's profit and the total treatment fees with subsidizing:

$$|F_2(\mathbf{x}^*_{M3}) - F_2(\mathbf{x}^*_{M1})| = |f'(\mathbf{x}^*_{M3}, \mathbf{y}^*_{M3}) - f(\mathbf{x}^*_{M1})| + ES, \tag{35}$$

where the terms $-f(\mathbf{x}^*_{M1})$ and $-F_2(\mathbf{x}^*_{M1})$ represent the carrier's profit and the total treatment fees, respectively, without any subsidies. These values are derived from solving model **[M1]**. When high-quality subsidies are applied (corresponding to model **[M3]**), the carrier's

profit and the total treatment fees are $-f'(\mathbf{x}^*_{M3}, \mathbf{y}^*_{M3})$ and $-F_2(\mathbf{x}^*_{M3})$, respectively. Therefore, $|F_2(\mathbf{x}^*_{M3}) - F_2(\mathbf{x}^*_{M1})|$, $|f'(\mathbf{x}^*_{M3}, \mathbf{y}^*_{M3}) - f(\mathbf{x}^*_{M1})|$, ES represent the government subsidies, ineffective subsidies (i.e., increase in the carrier's profit), and effective subsidies, respectively.

To avoid ineffective subsidies, we define the Effective Subsidy Rate (ESR) as an index to evaluate the performance of model **[M3]** in achieving the objective function F_2. The ESR ranges from $(0, 1]$, with values closer to 1 indicating a more effective subsidy scheme. The ESR is defined as follows:

$$\begin{aligned} ESR &= \frac{ES}{|F_2(\mathbf{x}^*_{M3}) - F_2(\mathbf{x}^*_{M1})|} \times 100\% \\ &= \frac{|F_2(\mathbf{x}^*_{M3}) - F_2(\mathbf{x}^*_{M1})| - |f'(\mathbf{x}^*_{M3}, \mathbf{y}^*_{M3}) - f(\mathbf{x}^*_{M1})|}{|F_2(\mathbf{x}^*_{M3}) - F_2(\mathbf{x}^*_{M1})|} \times 100\%. \end{aligned} \tag{36}$$

5. Case study in Chengdu

5.1. Experiment settings

We conduct numerical experiments using real data from Chengdu. Chengdu is one of China's new first-tier cities with a resident population of over 20 million. Currently, there are more than 15,000 trucks in Chengdu city. Fig. 4 shows the frequency distribution of the number of trucks owned by enterprises, with most enterprises owning fewer than 100 trucks.

[Figure 4 near here]

According to study Han et al. (2023), we consider a large case of 240 trucks that serves 30 sites in Longquanyi District, Chengdu (see Fig. 5), including 17 production sites, 10 backfill sites, and 3 processing facilities. We review government statistical reports and interview the carrier to collect the parameters for the experiment. There are mainly 4 sets of parameters in use, i.e., travel time-related, cost-related parameters, pollution-related, and hybrid approach-related. The values of these parameters are depicted in Appendix B and are explained below:

[Figure 5 near here]

The distance d between each site is obtained via the AMap (2025). We take a planning period of 10 hours with a time interval $\Delta t = 10$ minutes, resulting in $T = 60$ planning periods. It is difficult to accurately measure the traveling time between sites due to the uncertainty of traffic conditions on the road, so it is usually approximated by the average state in practice (Chu et al., 2012; Yazdani et al., 2021). The average speed of a truck traveling in Chengdu is set as $u = 30$ kilometer per hour. Therefore, the travel time between sites is calculated as $\overline{r}_{i,j} = \frac{d_{i,j}}{u}$ minutes, $i, j \in \{0\} \cup \mathcal{P} \cup \mathcal{S} \cup \mathcal{D}$. To ensure sufficient time redundancy, we set the traveling time as an integer multiple of the time interval Δt and round upwards, i.e. $r_{i,j} = \left\lceil \frac{\overline{r}_{i,j}}{\Delta t} \right\rceil$, so the number of planning periods is now approximately $\overline{T} = \max\{r_{i,j}\} + 1$, $i, j \in \{0\} \cup \mathcal{P} \cup \mathcal{S} \cup \mathcal{D}$. The time to load/unload a truck load of CW is usually 2-5 minutes, depending on the uncertain operating conditions. By Chu et al., we set the maximum number of load/unload operations per time interval Δt at the production site, backfill site, and processing facility to 2, 3, and 3, respectively.

We consider both diesel and electrical truck fleets. Han et al. (2023) explores the cost components of trucks in detail. For a diesel truck with an age of 5 years, fixed cost = purchase cost + maintenance cost - residual value = 987,000 + 149,000 - 185,000 = 951,000 CNY, then the average daily fixed cost = 951,000/365/5 = 521 CNY. Adding the driver's salary, we set the fixed cost of the daily operation of diesel trucks as $C_{0,v} = 750$ CNY, $v \in \mathcal{F}_d$. For an electrical truck, the purchase cost, maintenance cost, and residual value during the operation period of 5 years are 521,000, 196,000, and 100,000 CNY, respectively. The driver's salary is the same as that of the diesel truck, so the daily fixed cost of the electrical truck

is calculated as $C_{0,v} = 550$ CNY, $v \in \mathcal{F}_e$. The diesel price in Chengdu city is 7.8 CNY per liter, and the truck consumes 50 liters of fuel for 100 kilometers, so the cost of traveling for a time interval Δt is calculated as $C_{1,v} = 19.5$ CNY, $v \in \mathcal{F}_d$. The night-time price of electricity is 0.4 CNY per kilowatt hour (kWh), while the daytime price is 1.5 CNY per kWh. We therefore take the average price of electricity as 0.95 CNY per kWh. The electrical truck consumes 200 kWh for 100 kilometers, so the cost of traveling for a time interval Δt is calculated as $C_{1,v} = 9.5$ CNY, $v \in \mathcal{F}_e$. The transport price and treatment fee of CW are dynamically adjusted in practice, and there are no robust pricing standards in Chengdu. Through consultation with practitioners in the construction industry, it is known that the average transport price of CW is 20-30 CNY per tonne, and the treatment fee is 3-7 CNY per tonne. Therefore, we set the transport price $C_2 = 25$ CNY per tonne, and the market price for treatment fee $y' = 5$ CNY per tonne. The volume of CW produced is difficult to obtain, so we make reasonable assumptions based on publicly available data. According to the government statistics report (Chengdu Urban Management Committee and CAUPD, 2024), the Longquanyi District in Chengdu City produces approximately 180,000 tonnes of CW per day, with each production site generating an average of 900 tonnes of CW. Therefore, we set the daily production and backfill from construction sites as a normal distribution with a mean of 900 and a standard deviation of 100.

For further details on the parameters of electric and diesel trucks, refer to Truck Home (2024a) and Truck Home (2024b), respectively. Emission model parameters are from Barth et al. (2005) and presented in Table B1. We assume the acceleration τ and road angle δ are both 0 based on regional traffic conditions(Barth et al., 2005; Demir et al., 2011). Through consultation with practitioners in the construction industry, we set up three processing facilities to treat one tonne of CW resulting in pollution indices of $h_1 = 0.2, h_2 = 0.4, h_3 = 0.6$ respectively.

According to Soares et al. (2020), and after a large number of repeated experiments, we found that the following values of the parameters will lead to quick convergence. $\omega_0 = 0.8, \omega_1 = 0.1, \omega_2 = 0.1, M = 200, m = 10, p_m = 0.2, G' = 3, \sigma = 0.2, \epsilon = 0.001$. The number of particles $K = 40$. The upper-level objective function will not further improve usually after 20 iterations.

5.2. Computational performance

According to the parameter settings in Section 5.1, the lower level model [**M1**] contains 77,556 integer variables and 5,548 constraints. We implement the proposed hybrid approach on a laptop equipped with Intel(R) Core(TM) i9-10850K CPU at 3.6 GHz and 128 GB of RAM on a Windows 11 64-bit OS. We then discuss the model's performance for government and carrier separately.

5.2.1. Optimal strategy of the carrier

We solve model **[M1]** using the Gurobi solver (Gurobi Optimization, LLC, 2024), setting a time limit of 600 seconds. To assess the model's performance, we run 10 randomized experiments, with the results illustrating the variation of the model gap over time, as shown in Fig. 6. We observe that a high-quality solution (with a gap of less than 1%) can be obtained quickly, typically within 15 seconds. This is because the optimal solution of the original problem is close to the optimal solution of its linear relaxation. However, achieving a solution with a gap of less than 0.1% proves to be more time-consuming.

[Figure 6 near here]

In the experiment, we set the random seed to 42 and aim for a gap of less than 0.5%. The results are presented in Table 1. In this scenario, the total amount of CW at the production sites exceeds the demand at the backfill sites. As a result, trucks are tasked with transporting waste from the production sites to the processing facilities and backfill sites, but not from the

processing facilities to the backfill sites. A total of 105 trucks are in operation, consisting of 1 electric truck and 104 diesel trucks. As mentioned in Section 3, the carrier prefers using diesel trucks to maximize profit. The electric truck is only deployed when the diesel trucks reach full capacity.

[Table 1 near here]

Although the ideal method for evaluating the model's performance would involve comparing its results to current practices, complete real-world data is not available. Based on the analysis in Section 5.1, we estimate that the carrier requires 240 trucks to complete the transportation task. In contrast, the proposed approach only requires 105 trucks. This suggests that our method enhances transportation efficiency by 2 to 3 times.

5.2.2. Optimal strategy of the government

To assess the solution quality for model **[M3]**, we begin by solving model **[M2-HPR]** using the Gurobi solver. The solution of the high-point model represents the system's performance if all truck schedules are coordinated by the government. Under identical transportation tasks, the results in Table 2 show a 30.54% reduction in the pollution value ($\frac{11{,}723.23-8{,}142.39}{11{,}723.23}\times 100\% = 30.54\%$) in the HPR compared to model **[M1]**. However, this improvement in pollution control comes at a significant cost: the carrier's profit decreases substantially, from 230,242.50 CNY to 160,994.00 CNY.

[Table 2 near here]

We then apply the proposed method to solve model **[M3]**. In each run, we solve 800 integer programming subproblems (40 particles $\times$ 20 iterations). We set a GAP of 1% for each subproblem, and the total running time for the proposed method is 13,536 seconds (approximately 3.76 hours). Given that each planning period spans 10 hours, this solution time is acceptable. Fig. 7 illustrates the Pareto solution set of model **[M3]**. An interesting "jump" phenomenon is observed, where few feasible and Pareto optimal solutions for the pollution value lie in the interval $[8500, 9500]$. This occurs when the subsidy amount is insufficient to cover the additional cost of using electric trucks, leading the carrier to favor diesel trucks. However, once the subsidy surpasses this threshold, electric trucks become more attractive to the carrier than diesel trucks.

[Figure 7 near here]

The high-quality solution of model **[M3]** is the Pareto optimal solution with the minimum pollution value in Fig. 7. The results are shown in Table 3. The pollution value (primary objective function value) is 8,265.56, so $GAP\_F_1 = 1.51\%$ ($\frac{8{,}265.56-8{,}142.39}{8{,}142.39}\times 100\% = 1.51\%$). It shows that the proposed method finds a satisfactory solution for the pollution value. The secondary objective function value F_2 is 6,655.17, thus the effective subsidy rate $ESR = 95.74\%$ ($\frac{|6{,}655.17-(-35{,}375.00)|-|(-232{,}032.87)-(-230{,}242.50)|}{|6{,}655.17-(-35{,}375.00)|}\times 100\% = 95.74\%$), i.e., 95.74% of the government subsidies amount is used to reduce pollution. It shows that the proposed method finds a satisfactory solution for government subsidies. Therefore, we believe that the quality of the solution found by the proposed method is high and close to the global optimal solution.

[Table 3 near here]

According to Table 3, the carrier dispatches all 30 electrical trucks to transport 2,760 tonnes of waste and an additional 73 diesel trucks for 12,820 tonnes. The government subsidizes 42,000 CNY on the waste transportation process, which will reduce pollution by 29.49% ($\frac{11{,}723.23-8265.56}{11{,}723.23}\times 100\% = 29.49\%$). To further explore the operation regulations of the trucks, we examine Fig. 8. We observe some interesting phenomena: (1) Most production sites prioritize transporting waste to the nearest backfill sites. (2) When the closest site is occupied, the production site will opt for the second nearest backfill site. For instance, production site S_1 initially chooses backfill site D_1, but since D_1 is already assigned to handle waste from S_2, the waste from S_1 is instead shipped to D_2 to reduce waiting time. This scheduling approach

helps reduce congestion compared to manual methods. (3) The subsidies can incentivize the carrier to use electric trucks for long-distance waste transportation. For example, transportation to P_1 remain unchanged with or without the subsidies, but transportation to P_2 and P_3 shift from diesel trucks to electric trucks. This change occurs because P_2 and P_3 are further from surrounding production sites, making electric trucks a more economical option. Further analysis of important parameters is presented in Section 5.3.

[Figure 8 near here]

5.3. Sensitivity analysis

To understand the influence of the model parameters on the solution, a sensitivity analysis is conducted on the key parameters of the model, including the bounds of the treatment fee, the number of electrical trucks, and the truck speed.

5.3.1. Impact of the treatment fee

As a key parameter for policymaking, treatment fees directly influence pollution levels, government subsidies, and carrier profits (Huang et al., 2018). Therefore, we test different combinations of PUs and PLs to assess the sensitivity of the proposed model to treatment fees. In these tests, the values of PUs are drawn from the range of [3,7] with a step of 0.5 and PL is set as $PU - 10$ for each corresponding upper bound. The results are shown in Fig. 9.

As illustrated in Fig. 9 (a), pollution levels remain relatively stable across different $[PL, PU]$ intervals, indicating strong robustness of the model under varying policy settings. Fig. 9 (b) shows a clear negative correlation between total treatment fees and carrier profits, which aligns with practical expectations. However, it is worth noting that a higher treatment fee upper bound, while reducing government subsidies, may compress carrier profits and increase the risk of illegal dumping. Recent studies have proposed the use of AI-based techniques to detect non-compliant behaviors during transportation, such as trajectory anomaly detection and illegal dumping hotspot identification (Gao et al., 2024; Yu and Han, 2025). Therefore, policymakers may set treatment fee intervals $[PL, PU]$ in conjunction with AI-powered enforcement tools and the experimental insights from this study (Fig. 9 (b)), enabling more targeted, adaptive, and effective regulatory strategies.

[Figure 9 near here]

5.3.2. Impact of the number of electrical trucks

Increasing the ratio of electrical trucks to the CW transportation system could potentially reduce emissions though at the price of higher cost. Based on the parameters in Section 5.1, we set the number of electrical trucks N_1 to [10, 50] with a step size of 10 and evaluate its effects.

Fig. 10 demonstrates the changes in the pollution value and the total treatment fees with different ratios of electrical trucks. Both the pollution value and the total treatment fees show an approximately linear relation with the number of trucks. The objective value of pollution is reduced by 1,059.73 or 9.04% ($\frac{1059.73}{11723.23} \times 100\% = 9.04\%$) with a 10% increase of electrical trucks. The government subsidies, on the other hand, increase by an average of 10,942.50 (CNY). Therefore, increasing the number of electrical trucks can significantly reduce pollution though may incur higher costs. In addition, the rapid advancement of autonomous driving technology presents promising opportunities for its application in CW transportation (Hu et al., 2024). Given that such tasks typically involve fixed and repetitive routes, autonomous electric trucks have the potential to enhance transportation safety, operational stability, and environmental performance.

[Figure 10 near here]

5.3.3. Impact of the truck speed

The average truck speed u influences transportation efficiency, emissions, carrier profits, and hence government subsidies. In urban environments, truck speeds vary significantly between peak and off-peak hours. According to AMap (2025), vehicle speeds in downtown Chengdu typically range from 20 to 45 km/h. Based on this, we conduct a sensitivity analysis using $u = \{20, 25, 30, 35, 40, 45\}$, focusing on two objectives: pollution level (F_1 in model [M3]) and total treatment fees (i.e., $-F_2$).

As shown in Fig. 11, when u increases from 20 to 40 km/h, the pollution level drops significantly from about 9,100 to 7,550. This may result from two factors. First, higher speeds improve operational efficiency, enabling electric trucks to handle more waste and thus reducing reliance on diesel trucks. Second, as observed in Demir et al. (2014), fuel consumption per kilometer generally decreases with increasing speed at lower ranges, before rising again beyond a certain threshold. This explains the slight rebound in pollution when speed increases from 40 to 45 km/h, likely due to higher fuel consumption by diesel trucks. Regarding government expenditure, the total treatment fees remain relatively stable in the [20, 40] range, indicating low sensitivity. However, when the speed increases to 45 km/h, the total treatment fees decrease significantly. This is likely because higher speeds allow electric trucks to transport more waste within the same period, leading to greater government subsidies.

In summary, at a truck speed of 40 km/h, both pollution and government subsidies are lower. This aligns with typical night-time traffic speeds in Chengdu. Thus, prioritizing CW transportation during night hours could ease daytime congestion and improve environmental and economic performance. Additionally, GPS data and AI technologies (e.g., route tracking, speed prediction) can support real-time monitoring of truck compliance with time and speed regulations, enabling precise supervision and adaptive decision-making (Gao et al., 2024).

[Figure 11 near here]

6. Conclusions

This study investigates the strategic interaction between the government and the carrier in the context of CW transportation and proposes a bi-level optimization framework that incorporates practical constraints and policy interventions. We first develop a customized multi-vehicle minimum-cost flow model to maximize carrier profit without subsidies. Building on this, we construct a bi-level mixed-integer model where the government sets treatment fees to minimize pollution and subsidy expenditure. To solve this computationally challenging model, we design a hybrid algorithm based on MOPSO, where the upper level is handled by MOPSO and the lower level is efficiently solved using a commercial solver.

A large-scale case study in Chengdu demonstrates that the proposed method yields high-quality solutions within a reasonable time (3.76 hours), achieving a solution gap of 1.51%. Results show that an appropriate subsidy scheme can reduce emissions by 29.49%. The main findings and managerial insights are as follows:

1) The scheduling scheme prioritizes the nearest available processing or backfill site. When the closest site is congested, the system reroutes to the second best option, effectively alleviating local congestion;

2) A well-designed subsidy mechanism can improve transportation efficiency by 2–3 times. Without subsidies, diesel trucks are preferred; with subsidies, electric trucks become more cost-effective, especially for medium- and long-distance routes;

3) The carrier's profit is positively correlated with the government subsidies. By adjusting the treatment fees strategically, the government can intervene in the carrier's transportation schedule.

4) Increasing the proportion of electric trucks significantly reduces pollution. However, their high purchase and operating costs necessitate government subsidies;

5) Truck travel speed substantially affects system outcomes. Extremely low or high speeds hinder both pollution reduction and subsidy efficiency. For example, in Chengdu, maintaining an average speed of around 40 km/h is desirable.

The proposed model is flexible and extensible to more complex scenarios, such as multiple CW types (Appendix C). While we strive to align modeling assumptions and parameters with real-world settings, some limitations remain. First, the model assumes a fixed truck speed, which may not fully capture real-time traffic dynamics. Future research could incorporate uncertainty modeling and AI-based traffic prediction to improve robustness. Second, due to limited access to detailed operational data, empirical validation remains a challenge. Field studies with accurate real-world data are encouraged to further test and refine the model. Third, integrating our framework with emerging AI technologies—such as route tracking, violation detection, and autonomous electric trucks—may enable more precise regulation and adaptive decision-making. Finally, although this study focuses on model formulation and policy design, future work could explore the development of exact solution algorithms to enhance computational accuracy and scalability.

Disclosure statement

No potential conflict of interest was reported by the author(s).

Availability of the data

The datasets that support the findings of this study are available on request.

Funding

This work was supported by the National Natural Science Foundation of China under Grants no. 72101215 and 72071163; the Natural Science Foundation of Sichuan Province under Grant no. 2022NSFSC1906; and Technology Innovation and Development Project of Chengdu Science and Technology Bureau under Grant no. 2022-YF05-00839-SN.

References

Maziar Yazdani, Kamyar Kabirifar, Boadu Elijah Frimpong, Mahdi Shariati, Mirpouya Mirmozaffari, and Azam Boskabadi. Improving construction and demolition waste collection service in an urban area using a simheuristic approach: A case study in Sydney, Australia. *Journal of Cleaner Production*, 280:124138, 2021.

Zhuangqin Lin, Qiu Xie, Yingbin Feng, Peng Zhang, and Ping Yao. Towards a robust facility location model for construction and demolition waste transfer stations under uncertain environment: The case of Chongqing. *Waste management*, 105:73–83, 2020.

Beijia Huang, Xiangyu Wang, Harnwei Kua, Yong Geng, Raimund Bleischwitz, and Jingzheng Ren. Construction and demolition waste management in China through the 3r principle. *Resources, Conservation and Recycling*, 129:36–44, 2018.

Jiayuan Zheng, Ruwen Tan, Minjiu Yu, Zihan Tang, and Jing Zhang. Optimal decisions of construction and demolition waste recycling based on reference green effect under different subsidy models. *Computers & Industrial Engineering*, 196:110479, 2024.

Pradeep Rathore and Sarada Prasad Sarmah. Economic, environmental and social optimization of solid waste management in the context of circular economy. *Computers & Industrial Engineering*, 145:106510, 2020.

James C Chu, Shangyao Yan, and Kuan-Lin Chen. Optimization of earth recycling and dump truck dispatching. *Computers & Industrial Engineering*, 62(1):108–118, 2012.

Lei Yu and Ke Han. Using construction waste hauling trucks' gps data to classify earthwork-related locations: A chengdu case study. *IEEE Transactions on Big Data*, 2025.

Weisheng Lu, Chris Webster, Yi Peng, Xi Chen, and Xiaoling Zhang. Estimating and calibrating the amount of building-related construction and demolition waste in urban China. *International Journal of Construction Management*, 17(1):13–24, 2017.

José-Luis Gálvez-Martos, David Styles, Harald Schoenberger, and Barbara Zeschmar-Lahl. Construction and demolition waste best management practice in Europe. *Resources, conservation and recycling*, 136:166–178, 2018.

Shiv Sai Trivedi, K Snehal, BB Das, and Salim Barbhuiya. A comprehensive review towards sustainable approaches on the processing and treatment of construction and demolition waste. *Construction and Building Materials*, 393:132125, 2023.

Xinyuan Chen, Wen Yi, Hongping Yuan, and Weiwei Wu. Construction and demolition waste disposal charging scheme design. *Computer-Aided Civil and Infrastructure Engineering*, 39 (2):222–241, 2024.

Jeroen Beliën, Liesje De Boeck, and Jonas Van Ackere. Municipal solid waste collection and management problems: a literature review. *Transportation Science*, 48(1):78–102, 2014.

Jaime Solís-Guzmán, Madelyn Marrero, Maria Victoria Montes-Delgado, and Antonio Ramírez-de Arellano. A spanish model for quantification and management of construction waste. *Waste management*, 29(9):2542–2548, 2009.

Carmen Llatas. A model for quantifying construction waste in projects according to the European waste list. *Waste management*, 31(6):1261–1276, 2011.

Beatriz C Guerra, Fernanda Leite, and Kasey M Faust. 4d-bim to enhance construction waste reuse and recycle planning: Case studies on concrete and drywall waste streams. *Waste Management*, 116:79–90, 2020.

Roberto Aringhieri, Maurizio Bruglieri, Federico Malucelli, and Maddalena Nonato. A special vehicle routing problem arising in the optimization of waste disposal: a real case. *Transportation Science*, 52(2):277–299, 2018.

Yong Wang, Zheng Wang, Xiangpei Hu, Guiqin Xue, and Xiangyang Guan. Truck–drone hybrid routing problem with time-dependent road travel time. *Transportation Research Part C: Emerging Technologies*, 144:103901, 2022a.

Sytske C Wijnsma, Dominique Olié Lauga, and L Beril Toktay. Treat, dump, or export? how domestic and international waste management policies shape waste chain outcomes. *Management Science*, 2023.

Yong Wang, Shouguo Peng, Xuesong Zhou, Monirehalsadat Mahmoudi, and Lu Zhen. Green logistics location-routing problem with eco-packages. *Transportation Research Part E: Logistics and Transportation Review*, 143:102118, 2020.

Yong Wang, Jiayi Zhe, Xiuwen Wang, Jianxin Fan, Zheng Wang, and Haizhong Wang. Collaborative multicenter reverse logistics network design with dynamic customer demands. *Expert Systems with Applications*, 206:117926, 2022b.

Wen Yi, Ying Terk Lim, Huiwen Wang, Lu Zhen, and Xin Zhou. Construction waste transportation planning under uncertainty: Mathematical models and numerical experiments. *Mathematics*, 12(19):3018, 2024.

Wei Bi, Weisheng Lu, Zhan Zhao, and Christopher J Webster. Combinatorial optimization of construction waste collection and transportation: A case study of Hong Kong. *Resources, Conservation and Recycling*, 179:106043, 2022.

Yong Wang, Qiong Jiang, Xu Guan, and Xiangyang Guan. Recycling channel design and coordination in a reverse supply chain with customer green preference. *Transportation Research Part E: Logistics and Transportation Review*, 179:103329, 2023.

Yong Wang, Siyu Luo, Jianxin Fan, and Lu Zhen. The multidepot vehicle routing problem with intelligent recycling prices and transportation resource sharing. *Transportation Research Part E: Logistics and Transportation Review*, 185:103503, 2024.

Jingru Li, Jian Zuo, Hong Guo, Gaihong He, and Han Liu. Willingness to pay for higher construction waste landfill charge: A comparative study in Shenzhen and Qingdao, China. *Waste Management*, 81:226–233, 2018.

Jane L Hao, Martin J Hills, and Vivian WY Tam. The effectiveness of Hong Kong's construction waste disposal charging scheme. *Waste Management & Research*, 26(6):553–558, 2008.

Jingru Li, Jian Zuo, Gang Wang, Gaihong He, and Vivian WY Tam. Stakeholders' willingness to pay for the new construction and demolition waste landfill charge scheme in Shenzhen: A contingent valuation approach. *Sustainable Cities and Society*, 52:101663, 2020.

Nehal Elshaboury, Abobakr Al-Sakkaf, Eslam Mohammed Abdelkader, and Ghasan Alfalah. Construction and demolition waste management research: A science mapping analysis. *International journal of environmental research and public health*, 19(8):4496, 2022.

Hongping Yuan and Jiayuan Wang. A system dynamics model for determining the waste disposal charging fee in construction. *European Journal of Operational Research*, 237(3): 988–996, 2014.

Shuwei Jia, Guangle Yan, Aizhong Shen, and Jun Zheng. Dynamic simulation analysis of a construction and demolition waste management model under penalty and subsidy mechanisms. *Journal of Cleaner Production*, 147:531–545, 2017.

Malachy Carey and Mark McCartney. Pseudo-periodicity in a travel-time model used in dynamic traffic assignment. *Transportation Research Part B: Methodological*, 37(9):769–792, 2003.

Emrah Demir, Tolga Bektaş, and Gilbert Laporte. The bi-objective Pollution-Routing Problem. *European Journal of Operational Research*, 232(3):464–478, 2014. ISSN 0377-2217.

Emrah Demir, Tolga Bektaş, and Gilbert Laporte. A comparative analysis of several vehicle emission models for road freight transportation. *Transportation Research Part D: Transport and Environment*, 16(5):347–357, 2011. ISSN 1361-9209.

Ravindra K Ahuja, Thomas L Magnanti, James B Orlin, et al. *Network flows: theory, algorithms, and applications*, volume 1. Prentice hall Englewood Cliffs, NJ, 1993.

Inês Soares, Maria João Alves, and Carlos Henggeler Antunes. A deterministic bounding procedure for the global optimization of a bi-level mixed-integer problem. *European Journal of Operational Research*, 291(1):52–66, 2021.

Ankur Sinha, Pekka Malo, and Kalyanmoy Deb. A review on bilevel optimization: From classical to evolutionary approaches and applications. *IEEE transactions on evolutionary computation*, 22(2):276–295, 2017.

Inês Soares, Maria João Alves, and Carlos Henggeler Antunes. Designing time-of-use tariffs in electricity retail markets using a bi-level model - Estimating bounds when the lower level problem cannot be exactly solved. *Omega*, 93:102027, 2020.

C.A.C. Coello, G.T. Pulido, and M.S. Lechuga. Handling multiple objectives with particle swarm optimization. *IEEE Transactions on Evolutionary Computation*, 8(3):256–279, 2004.

James Kennedy and Russell Eberhart. Particle swarm optimization. In *Proceedings of ICNN'95-international conference on neural networks*, volume 4, pages 1942–1948. ieee, 1995.

Jing Liu, Jiajia Nie, and Hongping Yuan. To expand or not to expand: A strategic analysis of the recycler's waste treatment capacity. *Computers & Industrial Engineering*, 130:731–744, 2019.

James T Moore and Jonathan F Bard. The mixed integer linear bilevel programming problem. *Operations research*, 38(5):911–921, 1990.

Ke Han, Zhuoqian Yang, Caiyun Chen, Xiaobo Liu, Bin Zhao, Wei Li, and Yongdong Wang. Research on digital intelligent supervision and carbon reduction of construction waste trucks: A Chengdu case study (in Chinese), 12 2023. https://www.researchgate.net/publication/376354707_jianzhulajicheshuzhihuajianguanhejianwujiangtanyanjiu-yichengdoushiweili.

AMap. AMap API. https://lbs.amap.com/api/javascript-api, 2025.

Chengdu Urban Management Committee and CAUPD. Special plan for construction waste pollution prevention and control in Chengdu (2025-2035) (in Chinese). Technical report, Chengdu Urban Management Committee, Chengdu, China, 2024.

Truck Home. China national heavy duty truck HOWO TX 8X4 5.6m pure electric construction waste hauling trucks (in Chinese). [Online], 2024a. https://product.360che.com/m739/184872_index.html.

Truck Home. China national heavy duty truck HOWO TH7 550 HP 8X4 8.2m construction waste hauling trucks (in Chinese). [Online], 2024b. https://product.360che.com/m484/121055_index.html.

Matthew Barth, Theodore Younglove, and George Scora. Development of a heavy-duty diesel modal emissions and fuel consumption model. Technical report, California PATH Research Report, 2005.

Gurobi Optimization, LLC. Gurobi Optimizer Reference Manual, 2024. URL https://www.gurobi.com.

Yu Gao, Jiayuan Wang, and Xiaoxiao Xu. Machine learning in construction and demolition waste management: Progress, challenges, and future directions. *Automation in Construction*, 162:105380, 2024.

Qiaolin Hu, Weihua Gu, Lingxiao Wu, and Le Zhang. Optimal autonomous truck platooning with detours, nonlinear costs, and a platoon size constraint. *Transportation research part E: logistics and transportation review*, 186:103545, 2024.

Appendix A. Table of notations

Table A1: Summary of notation.

Sets	
$\{0\}$	Depot
$\mathcal{P}$	Processing facilities $\mathcal{P} = \{1, ..., P\}$
$\mathcal{S}$	Production sites $\mathcal{S} = \{P+1, ..., P+S\}$
$\mathcal{D}$	Backfill sites $\mathcal{D} = \{P+S+1, ..., P+S+D\}$
$\mathcal{T}$	Planning period $\mathcal{T} = \{0, 1, ..., T\}$
$\overline{\mathcal{T}}$	Virtual planning period $\overline{\mathcal{T}} = \{-1, ..., -\overline{T}\}$, $\overline{T} = \max\{r_{i,j}\} + 1$
$\mathcal{G}$	Time-space network $\mathcal{G} = \{\mathcal{N}, \mathcal{A}\}$, where $\mathcal{N}$ is the set of nodes and $\mathcal{A}$ is the set of arcs
$\mathcal{A}^f$, $\mathcal{A}^d$	Set of fully loaded arcs, set of deadheading arcs
$\mathcal{A}^s$, $\mathcal{A}^0$	Set of service arcs, set of zero arcs
$\mathcal{F}_e$	Electrical truck fleets $\mathcal{F}_e = \{\mathcal{V}_1, ..., \mathcal{V}_E\}$
$\mathcal{F}_d$	Diesel truck fleets $\mathcal{F}_d = \{\mathcal{V}_{E+1}, ..., \mathcal{V}_{E+\overline{D}}\}, E + \overline{D} = V$
Parameters	
N_v	Total number of trucks in feet $v \in \mathcal{F}_e \cup \mathcal{F}_d$ (veh)
Q_v	Rated load weight per truck in fleet $v \in \mathcal{F}_e \cup \mathcal{F}_d$ (kilogram/veh)
$\overline{Q}_v$	Unloaded weight per truck in fleet $v \in \mathcal{F}_e \cup \mathcal{F}_d$ (kilogram/veh)
M_v	Total weight per truck in the feet $v \in \mathcal{F}_d$, $M_v = Q_v + \overline{Q}_v$ (kilogram/veh)
qs_i	Total weight of CW at production site $i \in \mathcal{S}$ during the planning period (tonne)
qd_j	Total weight of CW at backfill site $j \in \mathcal{D}$ during the planning period (tonne)
Δt	Time interval
$r_{i,j}$	Trucks take $r_{i,j}$ time intervals to travel from site i to area j for $i, j \in \{0\} \cup \mathcal{P} \cup \mathcal{S} \cup \mathcal{D}$
B_j	Maximum number of trucks allowed to be serviced during the time interval Δt in site $j \in \mathcal{P} \cup \mathcal{S} \cup \mathcal{D}$
$C_{0,v}$	Fixed cost per truck in fleet $v \in \mathcal{F}_e \cup \mathcal{F}_d$ (CNY/veh)
$C_{1,v}$	Average cost of driving a time interval Δt with unloaded and fully loaded trucks in fleet $v \in \mathcal{F}_e \cup \mathcal{F}_d$ (CNY)
C_2	Price of transporting a tonne CW (CNY/tonne)
y'	Market guide price of treatment fee (CNY/tonne)
$d_{i,j}$	Distance between site $i \in \{0\} \cup \mathcal{P} \cup \mathcal{S} \cup \mathcal{D}$ and $j \in \{0\} \cup \mathcal{P} \cup \mathcal{S} \cup \mathcal{D}$ (meter)
u	Speed of trucks (meter/second)
PU	Upper bound of treatment fee(CNY/tonne)
PL	Lower bound of treatment fee (CNY/tonne)
ξ	Fuel-to-air mass ratio
k	Engine friction factor (kilojoule/revolution/liter)
N	Engine speed (revolution/second)
V	Engine displacement (liter)
κ	Heating value of a typical diesel fuel (kilojoule/gram)
η	Efficiency parameter for diesel engines
η_t	Drive train efficiency of trucks
τ	Acceleration of trucks (meter/square second)
g	Gravitational acceleration (meter/square second)
δ	Road angle (degree)
f_a	Coefficient of aerodynamic drag

(continued on next page)

(continued)	
f_r	Coefficient of rolling resistance
φ	Air density (kilogram/square meter)
A	Frontal surface area of diesel CHTH (square meter)
θ	Conversion factor of fuel from gram/second to liter/second
h_j	Pollution factor, $j \in \mathcal{P}$
$\lambda, \gamma, \alpha, \beta$	$\lambda = \frac{\xi}{\kappa\theta}$, $\gamma = \frac{1}{1{,}000\eta_t\eta}$, $\alpha = \tau + g\sin\delta + gf_r\cos\delta$, $\beta = 0.5 f_a \varphi A$
Decision variables	
$x_{i,j,v,t}$	Total flow of feet $v \in \mathcal{F}_e \cup \mathcal{F}_d$ from $i \in \{0\} \cup \mathcal{P} \cup \mathcal{S} \cup \mathcal{D}$ to $j \in \{0\} \cup \mathcal{P} \cup \mathcal{S} \cup \mathcal{D}$ at time $t \in \mathcal{T} \cup \overline{\mathcal{T}}$ (veh)
$y_{j,v}$	Treatment fee of transporting CW via fleet $v \in \mathcal{F}_e \cup \mathcal{F}_d$ to processing facility $j \in \mathcal{P}$ for harmless treatment (CNY/tonne)

Appendix B. Table of partial parameter values

Table B1: Partial parameter values.

Parameter	Value	Parameter	Value
T	60	Δt	10 minutes
u	30 kilometers/hour	$C_{0,v}$	750 CNY, $v \in \mathcal{F}_d$; 550 CNY, $v \in \mathcal{F}_e$
$C_{1,v}$	19.5 CNY, $v \in \mathcal{F}_d$; 9.5 CNY, $v \in \mathcal{F}_e$	C_2	25 CNY
y'	5 CNY	θ	737
$\overline{Q}_v$	15,500 kilogram, $v \in \mathcal{F}_d$	M_v	31,000 kilogram, $v \in \mathcal{F}_d$
ξ	1	k	0.2 kilojoule/revolution/liter
N	32 revolution/second	V	12.54 liter
κ	44 kilojoule/gram	η	0.9
η_t	0.4	τ	0
g	9.81 meter/square second	δ	0
f_a	0.7	f_r	0.01
φ	1.2041 kilogram/square meter	A	8.9 square meter

Appendix C. Models considering multiple CW types

Here we consider one extension of the model when CW can be categorized as multiple types such as inert waste, non-inert non-hazardous waste, and hazardous waste (Chen et al., 2024). Different types of waste have different recycling methods and treatment fees. Specifically, we define $\mathcal{C}$ as the set of all types of CW, and $c \in \mathcal{C}$ is a certain type of CW, and $c = 0$ represents that the trucks run empty. We redefine the upper decision variable $y_{j,v}$ and the lower decision variable $x_{i,j,v,t}$ as $y_{j,v,c}$, $x_{i,j,v,t,c}$, respectively, $i, j \in \{0\} \cup \mathcal{P} \cup \mathcal{S} \cup \mathcal{D}$, $v \in \mathcal{F}_e \cup \mathcal{F}_d$, $t \in \mathcal{T} \cup \overline{\mathcal{T}}$, $c \in \mathcal{C}$. We define the models that consider multiple types of CW as model **[M4]** and model **[M5]**. Models **[M4]** and **[M5]** are consistent with the solution approach for models **[M2]** and **[M3]**, respectively.

[M4]

$$\begin{aligned}\text{Min } F_1'(\mathbf{x}'|\mathbf{y}) = &\sum_{c\in\mathcal{C}}\sum_{i\in\mathcal{P}\cup\mathcal{S}\cup\mathcal{D}}\sum_{j\in\mathcal{P}\cup\mathcal{S}\cup\mathcal{D}}\sum_{v\in\mathcal{F}_d}\sum_{t\in\mathcal{T}} kNV\lambda d_{i,j}x'_{i,j,v,t,c}/u \\ &+\sum_{c\in\mathcal{C}}\sum_{i\in\mathcal{P}\cup\mathcal{S}\cup\mathcal{D}}\sum_{j\in\mathcal{P}\cup\mathcal{S}\cup\mathcal{D}}\sum_{v\in\mathcal{F}_d}\sum_{t\in\mathcal{T}} \overline{Q}_v\gamma\lambda\alpha_{i,j}d_{i,j}x'_{i,j,v,t,c} \\ &+\sum_{c\in\mathcal{C}}\sum_{i\in\mathcal{S}}\sum_{j\in\mathcal{P}\cup\mathcal{D}}\sum_{v\in\mathcal{F}_d}\sum_{t\in\mathcal{T}} Q_v\gamma\lambda\alpha_{i,j}d_{i,j}x'_{i,j,v,t,c} \\ &+\sum_{c\in\mathcal{C}}\sum_{i\in\mathcal{P}}\sum_{j\in\mathcal{D}}\sum_{v\in\mathcal{F}_d}\sum_{t\in\mathcal{T}} Q_v\gamma\lambda\alpha_{i,j}d_{i,j}x'_{i,j,v,t,c} \\ &+\sum_{c\in\mathcal{C}}\sum_{i\in\mathcal{P}\cup\mathcal{S}\cup\mathcal{D}}\sum_{j\in\mathcal{P}\cup\mathcal{S}\cup\mathcal{D}}\sum_{v\in\mathcal{F}_d}\sum_{t\in\mathcal{T}} \beta\gamma\lambda d_{i,j}x'_{i,j,v,t,c}u^2 \\ &+\sum_{c\in\mathcal{C}}\sum_{i\in\mathcal{S}}\sum_{j\in\mathcal{P}}\sum_{v\in\mathcal{F}_e\cup\mathcal{F}_d}\sum_{t\in\mathcal{T}} h_jQ_vx'_{i,j,v,t,c};\end{aligned} \tag{C1}$$

Subject to:

$$y_{j,v,c} \geq PL, \forall j \in \mathcal{P}, \forall v \in \mathcal{F}_e \cup \mathcal{F}_d, \forall c \in \mathcal{C}; \tag{C2}$$

$$y_{j,v,c} \leq PU, \forall j \in \mathcal{P}, \forall v \in \mathcal{F}_e \cup \mathcal{F}_d, \forall c \in \mathcal{C}; \tag{C3}$$

where

$$\begin{aligned}\mathbf{x}' \in \arg\min\{f''(\mathbf{x},\mathbf{y}) = &\sum_{v\in\mathcal{F}_e\cup\mathcal{F}_d}\sum_{j\in\mathcal{P}\cup\mathcal{S}\cup D}\sum_{t\in\mathcal{T}} C_{0,v}x_{0,j,v,t,0} \\ &+\sum_{c\in\mathcal{C}}\sum_{v\in\mathcal{F}_e\cup\mathcal{F}_d}\sum_{i\in\mathcal{P}\cup\mathcal{S}\cup\mathcal{D}}\sum_{j\in\mathcal{P}\cup\mathcal{S}\cup\mathcal{D}}\sum_{t\in\mathcal{T}} C_{1,v}r_{i,j}x_{i,j,v,t,c} \\ &-\sum_{c\in\mathcal{C}}\sum_{v\in\mathcal{F}_e\cup\mathcal{F}_d}\sum_{i\in\mathcal{S}\cup\mathcal{P}}\sum_{j\in\mathcal{D}}\sum_{t\in\mathcal{T}} C_2Q_vx_{i,j,v,t,c} \\ &-\sum_{c\in\mathcal{C}}\sum_{v\in\mathcal{F}_e\cup\mathcal{F}_d}\sum_{i\in\mathcal{S}}\sum_{j\in\mathcal{P}}\sum_{t\in\mathcal{T}}(C_2-y_{j,v,c})Q_vx_{i,j,v,t,c}\};\end{aligned} \tag{C4}$$

Subject to:

$$\sum_{j\in\mathcal{P}\cup\mathcal{S}\cup\mathcal{D}}\sum_{t\in\mathcal{T}} x_{0,j,v,t,0} \leq N_v, \forall v \in \mathcal{F}_e \cup \mathcal{F}_d; \tag{C5}$$

$$\sum_{j\in\mathcal{P}\cup\mathcal{S}\cup\mathcal{D}}\sum_{t\in\mathcal{T}} x_{0,j,v,t,0} - \sum_{i\in\mathcal{P}\cup\mathcal{S}\cup\mathcal{D}}\sum_{t\in\mathcal{T}} x_{i,0,v,t,0} = 0, \forall v \in \mathcal{F}_e \cup \mathcal{F}_d; \tag{C6}$$

$$\begin{aligned}&\sum_{c\in\mathcal{C}}\sum_{i\in\{0\}\cup\mathcal{P}\cup\mathcal{S}\cup\mathcal{D}} x_{i,j,v,t-r_{i,j}-1,c} - \sum_{c\in\mathcal{C}}\sum_{i\in\{0\}\cup\mathcal{P}\cup\mathcal{S}\cup\mathcal{D}} x_{j,i,v,t,c} = 0, \\ &\forall j \in \mathcal{P}\cup\mathcal{S}\cup\mathcal{D}, \forall v \in \mathcal{F}_e\cup\mathcal{F}_d, \forall t \in \mathcal{T};\end{aligned} \tag{C7}$$

$$\sum_{c\in\mathcal{C}}\sum_{i\in\{0\}\cup\mathcal{P}\cup\mathcal{S}\cup\mathcal{D}}\sum_{v\in\mathcal{F}_e\cup\mathcal{F}_d} x_{i,j,v,t-r_{i,j},c} \leq B_j, \forall j \in \mathcal{P}\cup\mathcal{S}\cup\mathcal{D}, \forall t \in \mathcal{T}; \tag{C8}$$

$$\sum_{c\in\mathcal{C}}\sum_{j\in\mathcal{P}\cup\mathcal{D}}\sum_{v\in\mathcal{F}_e\cup\mathcal{F}_d}\sum_{t\in\mathcal{T}} Q_vx_{i,j,v,t,c}/1,000 = qs_i, \forall i \in \mathcal{S}; \tag{C9}$$

$$\sum_{c\in\mathcal{C}}\sum_{i\in\mathcal{P}\cup\mathcal{S}}\sum_{v\in\mathcal{F}_e\cup\mathcal{F}_d}\sum_{t\in\mathcal{T}} Q_vx_{i,j,v,t,c}/1,000 = qd_j, \forall j \in \mathcal{D}; \tag{C10}$$

$$x_{i,j,v,t,c} = 0, \forall i,j \in \{0\}\cup\mathcal{P}\cup\mathcal{S}\cup\mathcal{D}, \forall v \in \mathcal{F}_e\cup\mathcal{F}_d, \forall t \in \overline{\mathcal{T}}, \forall c \in \mathcal{C}; \tag{C11}$$

$$x_{i,j,v,t,c} = 0, \exists\mathcal{H} \in \{\{0\},\mathcal{P},\mathcal{S},\mathcal{D}\}, \forall i,j \in \mathcal{H}, \forall v \in \mathcal{F}_e\cup\mathcal{F}_d, \forall t \in \mathcal{T}, \forall c \in \mathcal{C}; \tag{C12}$$

$$x_{0,j,v,t,c} = 0, \forall j \in \{0\} \cup \mathcal{P} \cup S \cup D, \forall v \in \mathcal{F}_e \cup \mathcal{F}_d, \forall t \in \mathcal{T}, \forall c \in \mathcal{C} \backslash \{0\}; \tag{C13}$$

$$x_{i,0,v,t,c} = 0, \forall i \in \{0\} \cup \mathcal{P} \cup S \cup D, \forall v \in \mathcal{F}_e \cup \mathcal{F}_d, \forall t \in \mathcal{T}, \forall c \in \mathcal{C} \backslash \{0\}; \tag{C14}$$

$$\sum_{c \in \mathcal{C}} x_{i,j,v,t,c} \in \{0, 1, ..., B_j\}, \forall i, j \in \{0\} \cup \mathcal{P} \cup S \cup D, \forall v \in \mathcal{F}_e \cup \mathcal{F}_d, \forall t \in \mathcal{T} \cup \overline{\mathcal{T}}. \tag{C15}$$

[M5]

$$\text{Min} - \sum_{c \in \mathcal{C}} \sum_{i \in \mathcal{S}} \sum_{j \in \mathcal{P}} \sum_{v \in \mathcal{F}_e \cup \mathcal{F}_d} \sum_{t \in \mathcal{T}} y_{j,v,c} Q_v x'_{i,j,v,t,c}; \tag{C16}$$

Subject to:

$$F'_1(\mathbf{x}'|\mathbf{y}) = F'_1(\mathbf{x}^*_{M4}); \tag{C17}$$

Constraints (C2) – (C3);

where

$$\mathbf{x}' \in \arg\min\{f''(\mathbf{x}, \mathbf{y})\}; \tag{C18}$$

Subject to:

Constraints (C5)-(C15).

The solution approach of this model could be barely solved by the same routine as presented in Section 4.

List of Table

Table 1: Results of model **[M1]**

Parameters	Values
Objective value: profit of carrier (CNY)	230,242.50
Gap	0.37%
Runtime (second)	45
Total treatment fees (CNY)	35,375.00
Pollution value	11,723.23
Number of electrical trucks	1
Number of diesel trucks	104
Transport volume of electrical trucks (tonne)	70
Transport volume of diesel trucks (tonne)	15,570
Transport volume from $\mathcal{S}$ to $\mathcal{P}$ (tonne)	7,075
Transport volume from $\mathcal{S}$ to $\mathcal{D}$ (tonne)	8,565
Transport volume from $\mathcal{P}$ to $\mathcal{D}$ (tonne)	0
Total volume of CW (tonne)	15,640

Table 2: Results of model **[M2-HPR]**

Parameters	Values
Objective value: pollution value	8,142.39
Gap	0.43%
Runtime (second)	58
Profit of carrier (CNY)	160,994
Total treatment fees (CNY)	35,175
Number of electrical trucks	30
Number of diesel trucks	210
Transport volume of electrical trucks (tonne)	2,790
Transport volume of diesel trucks (tonne)	12,825
Transport volume from $\mathcal{S}$ to $\mathcal{P}$	7,035
Transport volume from $\mathcal{S}$ to $\mathcal{D}$	8,580
Transport volume from $\mathcal{P}$ to $\mathcal{D}$	0
Total volume of CW (tonne)	15,615

Table 3: Results of model **[M3]**

Parameters	Values
Primary objective F_1: pollution value	8,265.56
Secondary objective F_2: Opposite of total treatment fees (CNY)	6655.17
Runtime (second)	13,536 (3.76 hours)
Profit of carrier (CNY)	232,032.87
Number of electrical trucks	30
Number of diesel trucks	73
Transport volume of electrical trucks (tonne)	2,760
Transport volume of diesel trucks (tonne)	12,820
Transport volume from $\mathcal{S}$ to $\mathcal{P}$ (tonne)	7,025
Transport volume from $\mathcal{S}$ to $\mathcal{D}$ (tonne)	8,555
Transport volume from $\mathcal{P}$ to $\mathcal{D}$ (tonne)	0
Total volume of CW (tonne)	15,580
The gap of objective function F_1, GAP_F_1	1.51%
Effective subsidy rate, ESR	95.74%

List of figures

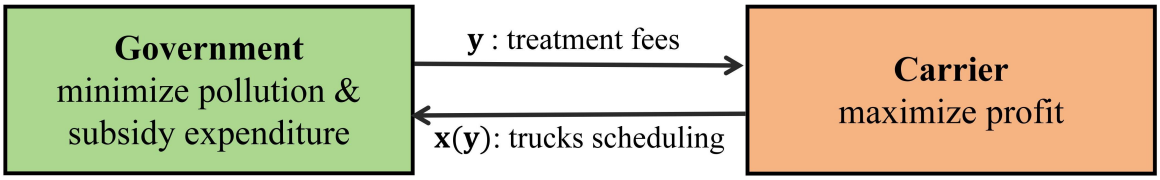

Figure 1: The structure of bi-level model.

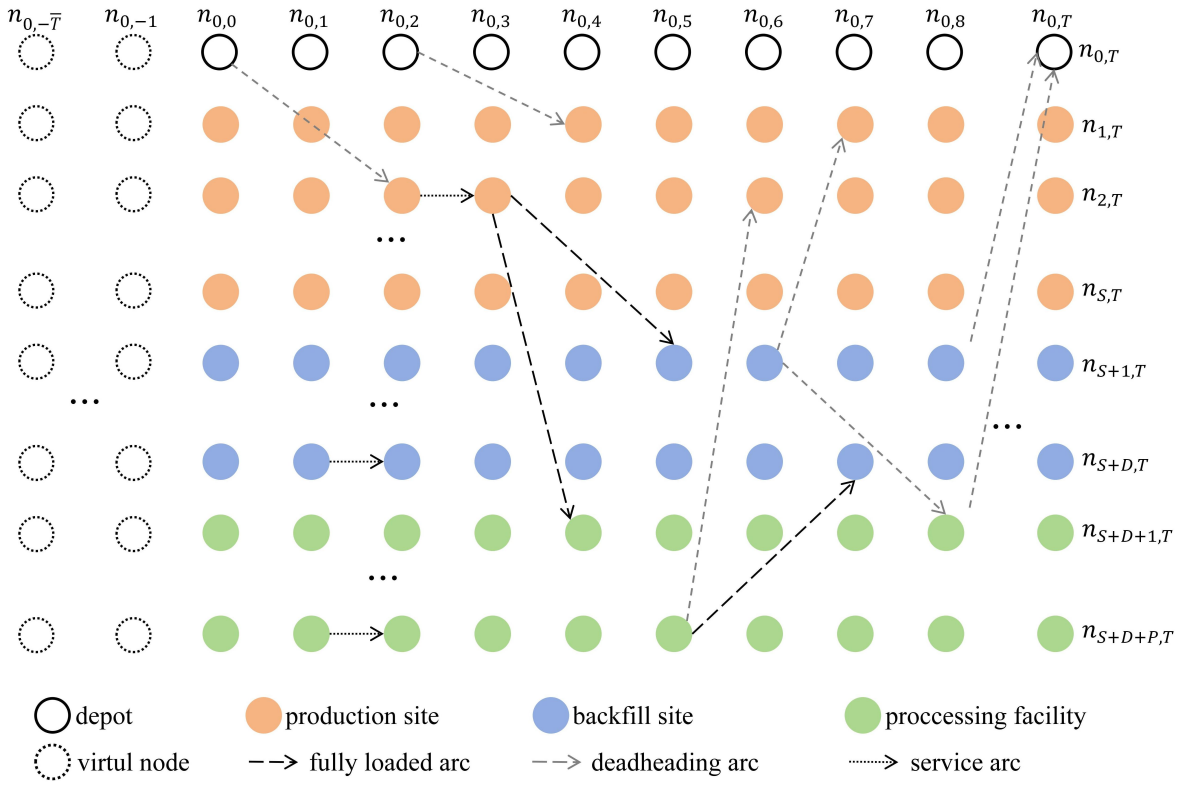

Figure 2: Time-space network $\mathcal{G}$.

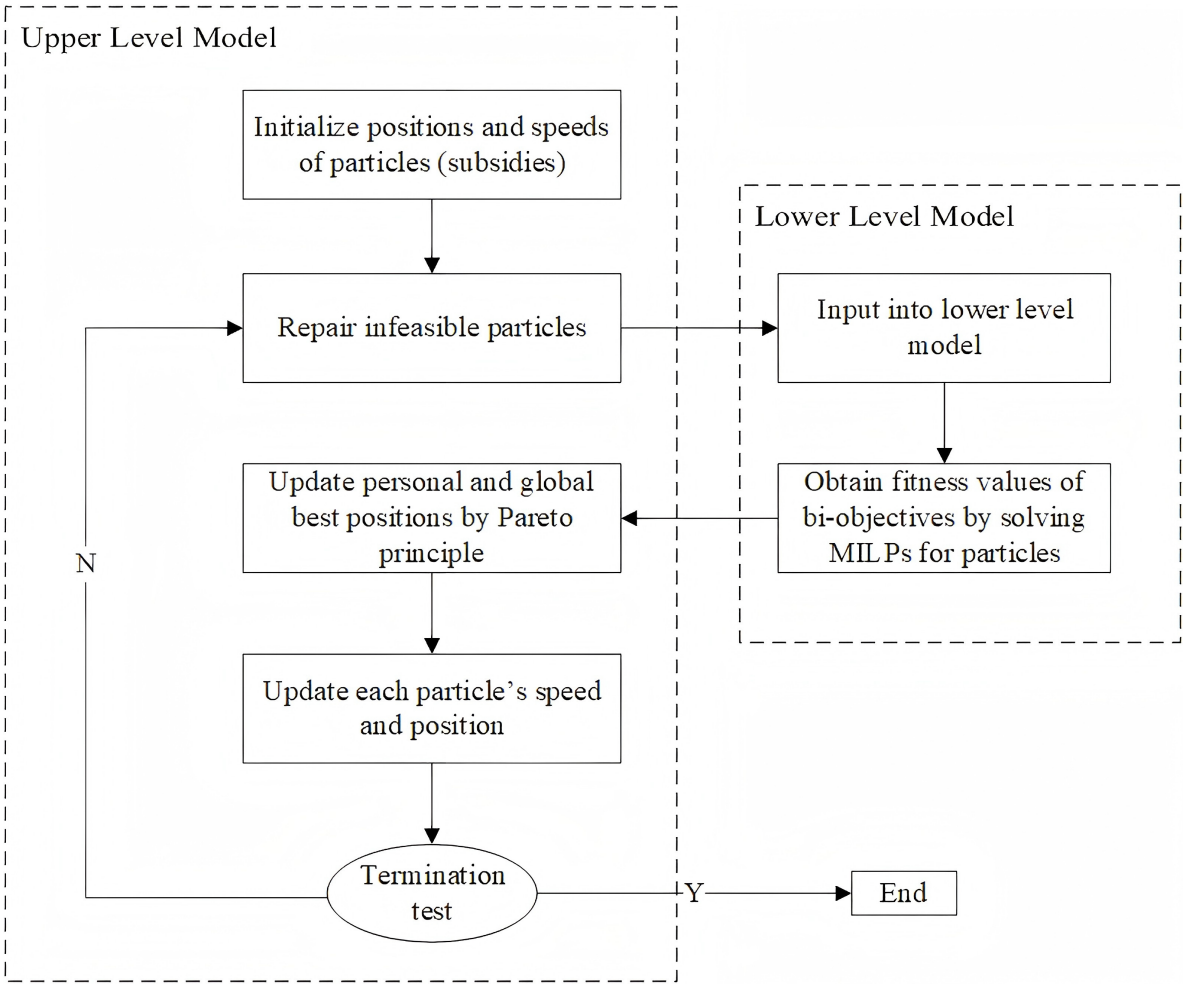

Figure 3: Hybrid algorithm flowchart.

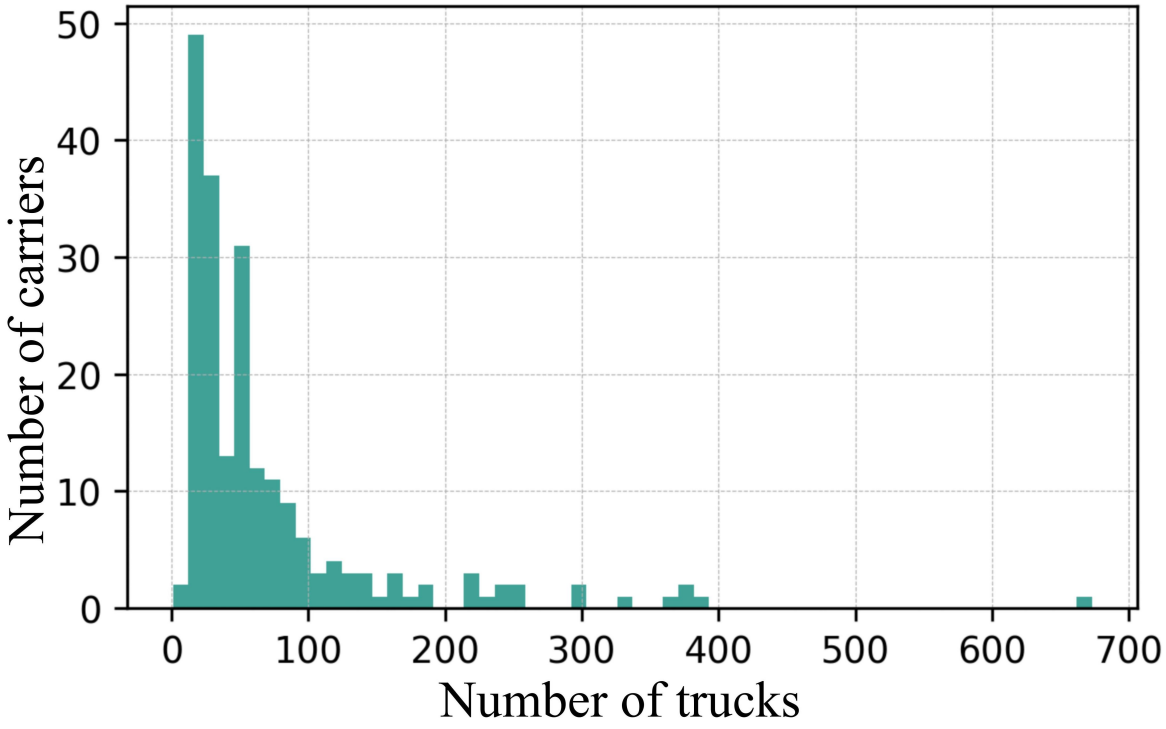

Figure 4: Frequency distribution of trucks held by carriers.

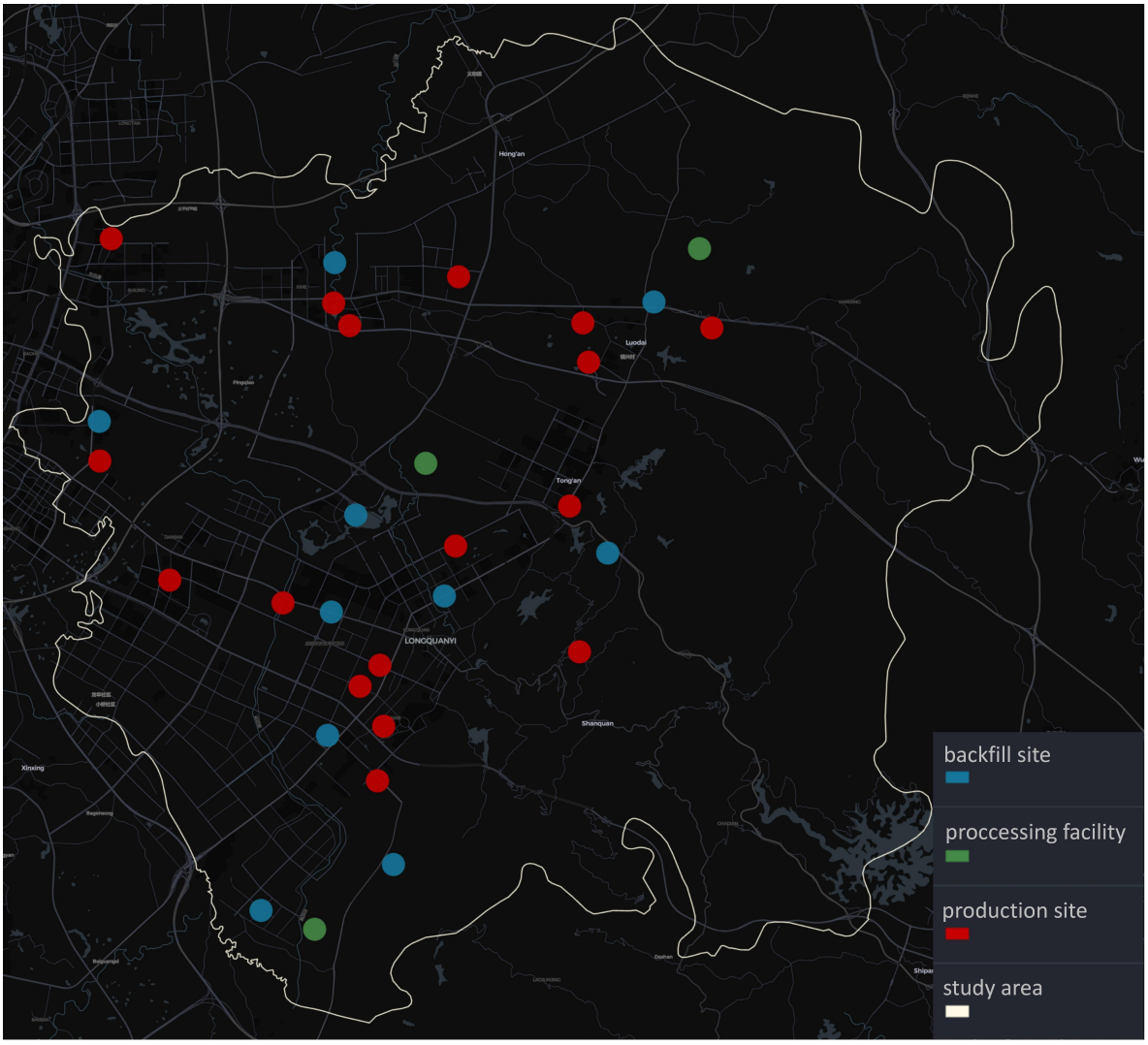

Figure 5: The location of sites.

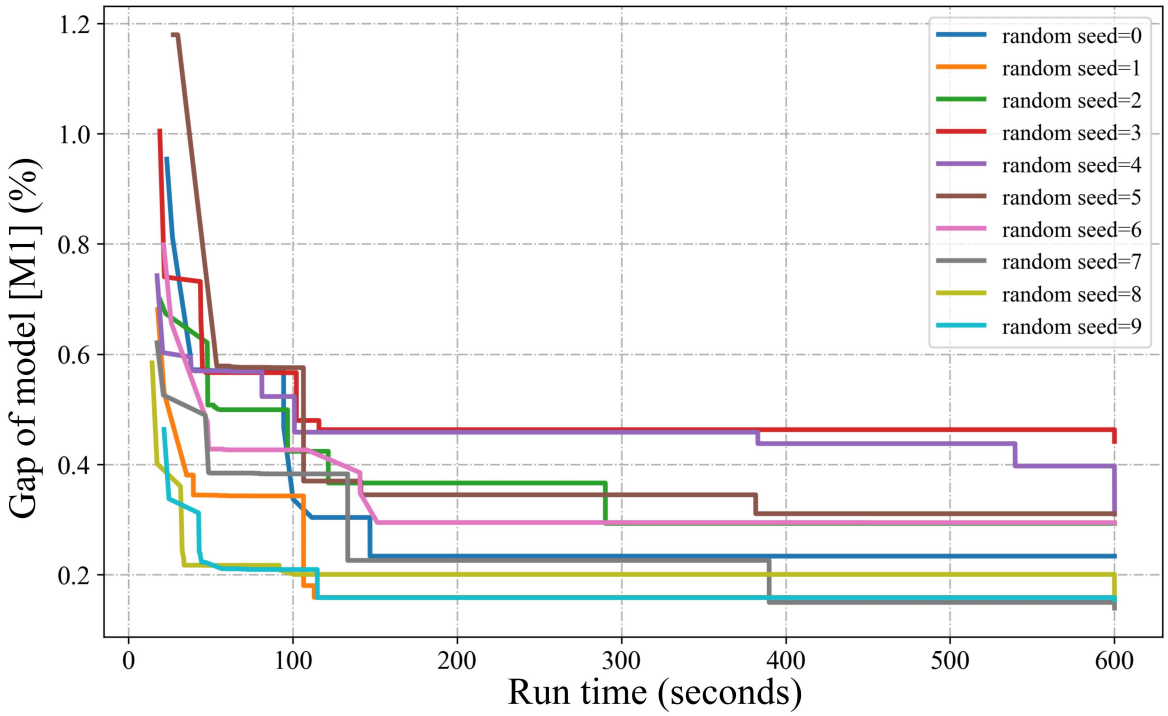

Figure 6: The variations of model gap with run time. Ten repetitions of the experiment for model **[M1]**.

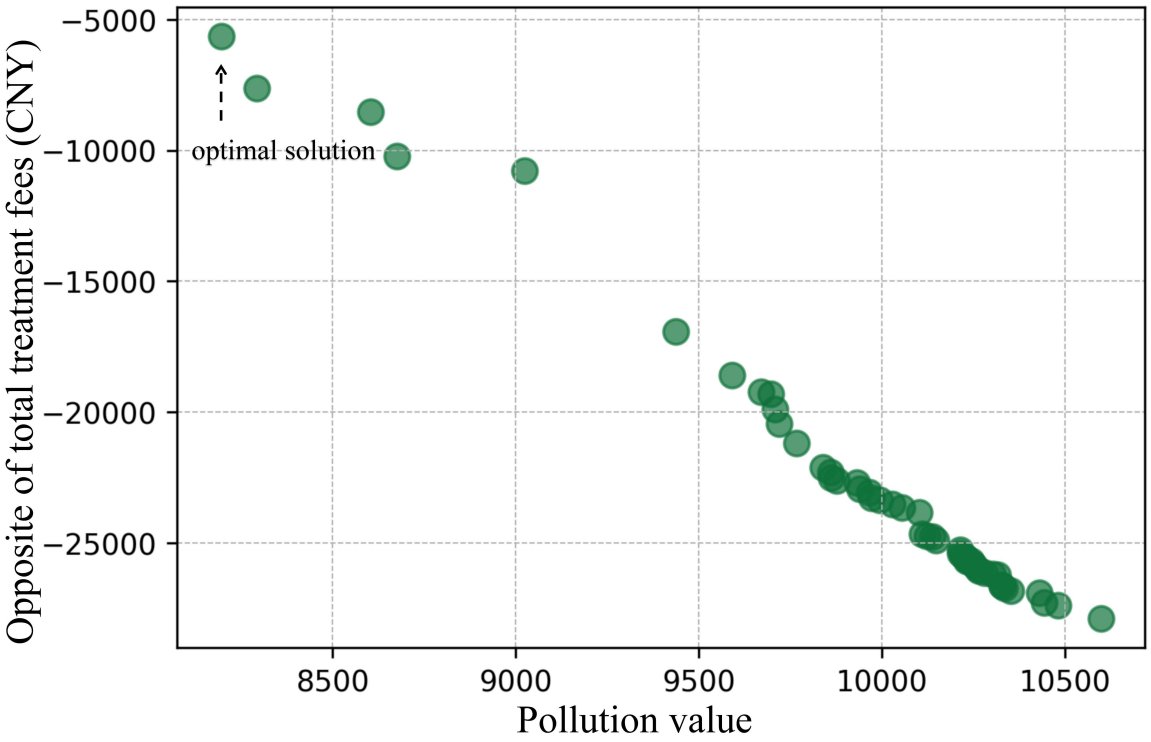

Figure 7: The Pareto optimal solution set of **[M3]**.

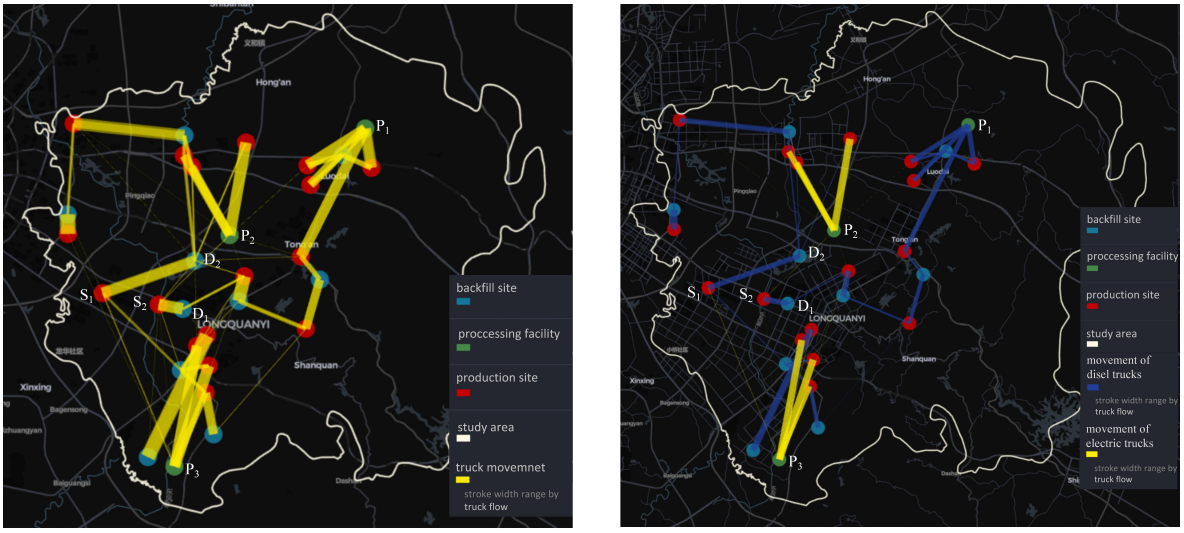

(a) Movement of CW

(b) Movement of electric and diesel trucks

Figure 8: Movement of CW and trucks between sites. (a) illustrates the flow of CW between each site in a planning period, where the stroke width of the arcs represents the amount of CW. (b) shows the movement of electrical and diesel trucks between each site in a planning period, where the stroke width of the arcs corresponds to the total number of trips.

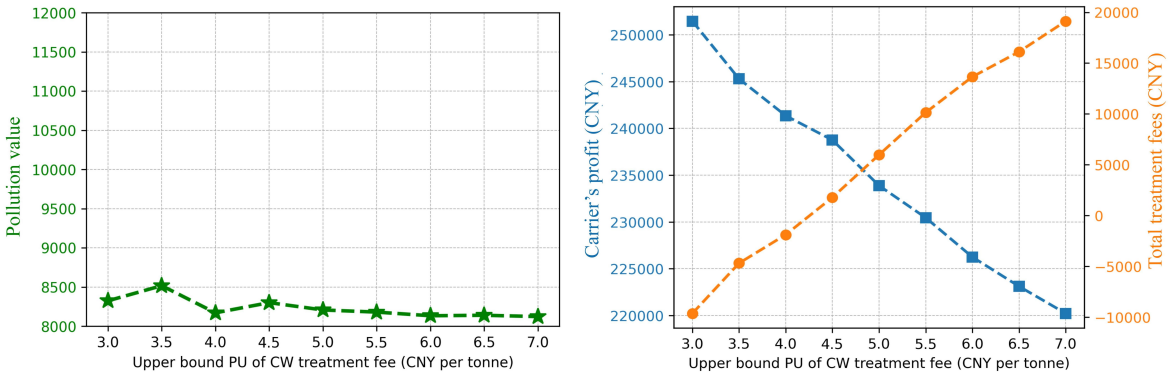

(a) Pollution value

(b) Total treatment fees and contractor's profit

Figure 9: Sensitivity of the treatment fee.

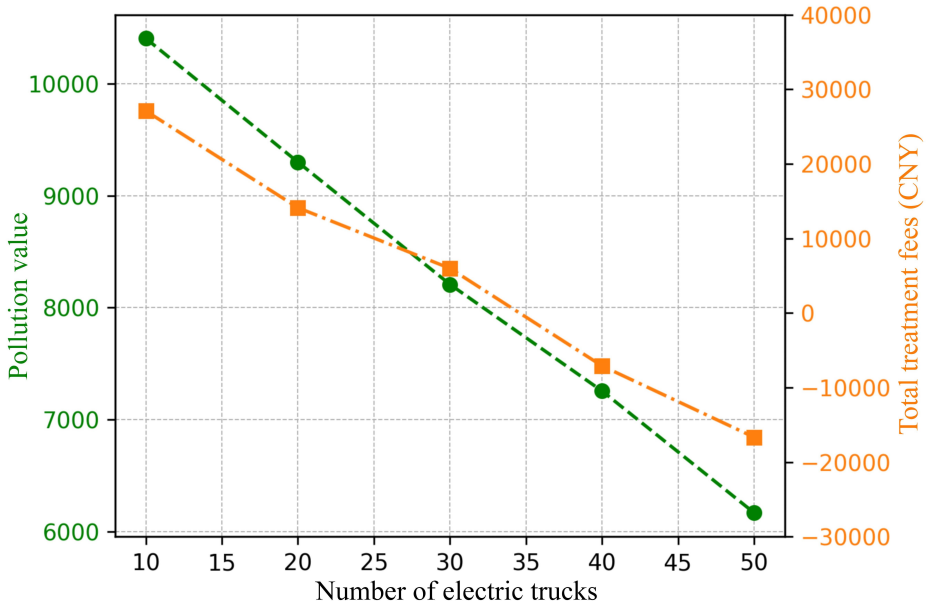

Figure 10: Sensitivity of the number of electrical trucks.

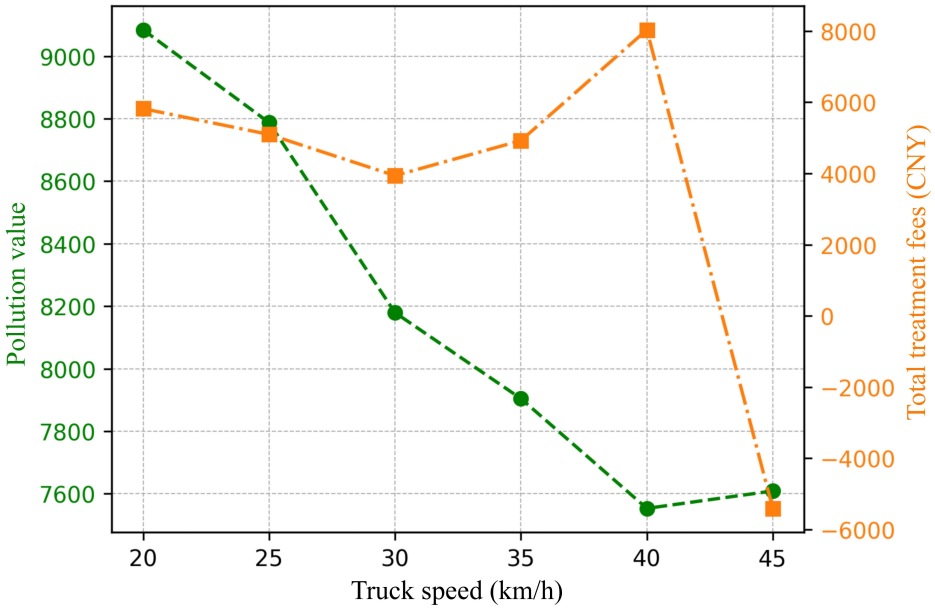

Figure 11: Sensitivity of the truck speed.